Eur. Phys. J. C (2022) 82:769
https://doi.org/10.1140/epjc/s10052-022-10639-9

THE EUROPEAN PHYSICAL JOURNAL C

Regular Article - Theoretical Physics

Fermion masses and mixings and $g-2$ muon anomaly in a 3-3-1 model with D_4 family symmetry

A. E. Cárcamo Hernández[1,2,3,a], **Hoang Ngoc Long**[4,5,b], **M. L. Mora-Urrutia**[1,c], **N. H. Thao**[6,d], **V. V. Vien**[7,8,e]

[1] Universidad Técnica Federico Santa María, Casilla 110-V, Valparaiso, Chile
[2] Centro Científico-Tecnológico de Valparaíso, Casilla 110-V, Valparaiso, Chile
[3] Millennium Institute for Subatomic Physics at High Energy Frontier-SAPHIR, Fernandez Concha 700, Santiago, Chile
[4] Center for Forecasting Studies, Thu Dau Mot University, Binh Duong Province, Vietnam
[5] Institute of Physics, Vietnam Academy of Science and Technology, 10 Dao Tan, Ba Dinh, Hanoi, Vietnam
[6] Department of Physics, Hanoi Pedagogical University 2, Phuc Yen, Vinh Phuc, Vietnam
[7] Institute of Applied Technology, Thu Dau Mot University, Thu Dau Mot, Binh Duong Province, Vietnam
[8] Department of Physics, Tay Nguyen University, 567 Le Duan, Buon Ma Thuot City, DakLak, Vietnam

Received: 24 November 2021 / Accepted: 26 July 2022 / Published online: 31 August 2022

Abstract We propose a predictive model based on the $SU(3)_C \times SU(3)_L \times U(1)_X$ gauge symmetry, which is supplemented by the D_4 family symmetry and several auxiliary cyclic symmetries whose spontaneous breaking produces the observed SM fermion mass and mixing pattern. The masses of the light active neutrinos are produced by an inverse seesaw mechanism mediated by three right handed Majorana neutrinos. To the best of our knowledge the model corresponds to the first implementation of the D_4 family symmetry in a $SU(3)_C \times SU(3)_L \times U(1)_X$ theory with three right handed Majorana neutrinos and inverse seesaw mechanism. Our proposed model successfully accommodates the experimental values of the SM fermion mass and mixing parameters, the muon anomalous magnetic moment as well as the Higgs diphoton decay rate and meson oscillations constraints. The consistency of our model with the muon anomalous magnetic moment requires charged exotic vector like leptons at the TeV scale.

1 Introduction

Despite its great success and consistency with the experimental data, Standard Model (SM) have several unexplained issues such as the number of SM fermion families, the electric charge quantization, the huge SM fermion mass hierarchy, the small quark mixing angles and the sizeable leptonic mixing ones. Whereas the quark mixing angles are small, two of the leptonic mixing angles are large and one is of the order of the Cabibbo angle. In addition, the SM charged fermion mass pattern spread over a range of 13 orders of magnitude from the light active neutrino mass scale up to the top quark mass. This is the so called flavour puzzle of the SM which motivates the construction of several extensions of the SM with augmented particle spectrum and extra symmetries, which be continuous and (or) discrete, introduced to provide a successful explanation of the observed SM fermion mass and mixing hierarchy. Discrete flavor symmetries have been shown to be successful in describing the SM fermion mass and mixing pattern. Some reviews of discrete flavor groups are provided in [1–4]. In particular, the D_4 discrete flavor group, which has a small amount of doublets and singlets in their irreducible representations has been employed in extensions of the SM [5–20], since it allows to get viable predictions for the SM fermion mass and mixing hierarchy, with a moderate amount of particle content. Furthermore, several theories with enlarged particle spectrum and symmetries have been constructed to explain the experimental value of the muon anomalous magnetic moment, anomaly recently confirmed by the muon $g-2$ experiment at FERMILAB. See [21] for a very recent review.

To address the aforementioned issues of the SM, in this paper, we construct a theory based on the $SU(3)_C \times SU(3)_L \times U(1)_X$ gauge symmetry (3-3-1 model) with extended particle spectrum and discrete symmetries which allows to get predictive SM fermion mass matrices consis-

[a] e-mail: antonio.carcamo@usm.cl
[b] e-mail: hoangngoclong@tdmu.edu.vn (corresponding author)
[c] e-mail: maria.luisa.mora.u@gmail.com
[d] e-mail: nguyenhuythao@hpu2.edu.vn
[e] e-mail: vovanvien@tdmu.edu.vn

tent with the low energy SM fermion flavor data. In our proposed theory, we considered the $SU(3)_C \times SU(3)_L \times U(1)_X$ gauge symmetry, since models having this symmetry naturally explain the number of SM fermion families as well as the electric charge quantization, see for instance [22–43] . Apart from successfully addressing these features, our proposed model also successfully explains and accommodates the SM fermion mass and mixing hierarchy the muon anomalous magnetic moment as well as the Higgs diphoton decay rate constraints. Our theory is based in the D_4 discrete symmetry, which is supplemented by several cyclic symmetries. In our proposed theory, the SM fermion mass and mixing pattern is produced by the spontaneous breaking of the discrete symmetries, whereas the tiny masses of the light active neutrinos are produced by an inverse seesaw mechanism mediated by three right handed Majorana neutrinos. To the best of our knowledge our work corresponds to the first implementation of the D_4 family symmetry in a $SU(3)_C \times SU(3)_L \times U(1)_X$ theory with three right handed Majorana neutrinos and inverse seesaw mechanism. The layout of the reminder of the paper is as follows. In Sect. 2 we describe the proposed model. The consequences of the model in quark masses and mixings are analyzed in Sect. 3. Lepton masses and mixings are described in Sect. 4. The low energy scalar of the model is discussed in Sect. 5. In Sect. 6 we discuss the implications of the model in the Higgs diphoton decay rate. The implications of the model in the muon anomalous magnetic and meson oscillations are discussed in Sects. 7 and 8. We conclude in Sect. 9.

2 The model

The model under consideration is based on the $SU(3)_C \times SU(3)_L \times U(1)_X$ gauge symmetry, which is supplemented by the $D_4 \times Z_4 \times Z_3^{(1)} \times Z_3^{(2)} \times Z_{16}$ discrete group, whose spontaneous breaking generates viable and predictive fermion mass matrices consistent with the observed pattern of SM fermion masses and mixings. We choose the D_4 symmetry since it is the smallest non-Abelian discrete symmetry group having five irreducible representations (irreps), explicitly, four singlets and one doublet irreps. The auxiliary cyclic symmetries Z_4, $Z_3^{(1)}$ and $Z_3^{(2)}$ select the allowed entries of the SM fermion mass matrices that yield a predictive and viable pattern of SM fermion masses and mixings. These cyclic symmetries also allows a successful implementation of the inverse seesaw mechanism. These symmetries together with the Z_{16} symmetry shape the hierarchical structure of the SM charged fermion mass matrices crucial to yield the observed pattern of SM charged fermion masses and mixing angles. Furthermore, the Z_{16} discrete symmetry is also crucial to get sufficiently suppressed non renormalizable mass terms involving gauge singlet right handed Majorana neutrinos, required for the implementation of the inverse seesaw mechanism that produces small masses for the light active neutrinos. The model fermionic sector contains $SU(3)_L$ fermionic triplets and antitriplets, transforming under the $SU(3)_C \times SU(3)_L \times U(1)_X$ gauge symmetry as follows:

$$
\begin{aligned}
&Q_{1L} = \begin{pmatrix} u_1 \\ d_1 \\ J_1 \end{pmatrix}_L \sim \left(\mathbf{3}, \mathbf{3}, \frac{1}{3}\right), \\
&Q_{nL} = \begin{pmatrix} d_n \\ -u_n \\ J_n \end{pmatrix}_L \sim \left(\mathbf{3}, \bar{\mathbf{3}}, 0\right), \\
&u_{iR} \sim \left(\mathbf{3}, \mathbf{1}, \frac{2}{3}\right), \quad d_{iR} \sim \left(\mathbf{3}, \mathbf{1}, -\frac{1}{3}\right), \\
&J_{1R} \sim \left(\mathbf{3}, \mathbf{1}, \frac{2}{3}\right), \quad J_{nR} \sim \left(\mathbf{3}, \mathbf{1}, -\frac{1}{3}\right), \\
&L_{iL} = \begin{pmatrix} \nu_i \\ l_i \\ \nu_i^c \end{pmatrix}_L \sim \left(\mathbf{1}, \mathbf{3}, -\frac{1}{3}\right), \; l_{iR} \sim (\mathbf{1}, \mathbf{1}, -1), \\
&N_{iR} \sim (\mathbf{1}, \mathbf{1}, 0), \; n = 2, 3; i = 1, 2, 3.
\end{aligned} \tag{1}
$$

All $SU(3)_L$ singlets $\{\xi, \Xi, \sigma, \phi_{1,2}, \Phi, \phi, \zeta, \eta, \varphi_{1,2}\}$ transform as $(\mathbf{1}, \mathbf{1}, 0)$ under the $SU(3)_C \times SU(3)_L \times U(1)_X$ gauge symmetry.

Furthermore, in the model fermionic sector, three right handed Majorana neutrinos are included as well, in order to allow a successful implementation of the inverse seesaw mechanism that produces the tiny active neutrino masses. Notice that the fermions in our model do not feature exotic electric charges, from which it follows that the electric charge is given by:

$$
Q = T_3 + \beta T_8 + X = T_3 - \frac{1}{\sqrt{3}} T_8 + X. \tag{2}
$$

On the other hand, the model scalar sector is composed of two $SU(3)_L$ triplet scalars χ and ρ and several gauge singlet scalar fields to be specified below. The $SU(3)_L$ scalar χ and ρ can be expanded around the minimum as follows:

$$
\begin{aligned}
\chi &= \begin{pmatrix} \chi_1^0 \\ \chi_2^- \\ \frac{1}{\sqrt{2}}(v_\chi + \xi_\chi \pm i\zeta_\chi) \end{pmatrix}, \\
\rho &= \begin{pmatrix} \rho_1^+ \\ \frac{1}{\sqrt{2}}(v_\rho + \xi_\rho \pm i\zeta_\rho) \\ \rho_3^+ \end{pmatrix}.
\end{aligned} \tag{3}
$$

This implies that the $SU(3)_L$ scalar triplets acquire the following VEV pattern:

$$
\begin{aligned}
\langle\chi\rangle^T &= \left(0, \quad 0, \quad v_\chi/\sqrt{2}\right), \\
\langle\rho\rangle^T &= \left(0, \quad v_\rho/\sqrt{2}, \quad 0\right).
\end{aligned} \tag{4}
$$

Table 1 Scalar transformations under the $SU(3)_C \times SU(3)_L \times U(1)_X \times D_4 \times Z_4 \times Z_3^{(1)} \times Z_3^{(2)} \times Z_{16}$ group

	χ	ρ	ξ	Ξ	σ	ϕ_1	ϕ_2	Φ	ζ	η	φ_1	φ_2
$SU(3)_C$	$\mathbf{1}$	$\mathbf{1}$	$\mathbf{1}$	$\mathbf{1}$	$\mathbf{1}$	$\mathbf{1}$	$\mathbf{1}$	$\mathbf{1}$	$\mathbf{1}$	$\mathbf{1}$	$\mathbf{1}$	$\mathbf{1}$
$SU(3)_L$	$\mathbf{3}$	$\mathbf{3}$	$\mathbf{1}$	$\mathbf{1}$	$\mathbf{1}$	$\mathbf{1}$	$\mathbf{1}$	$\mathbf{1}$	$\mathbf{1}$	$\mathbf{1}$	$\mathbf{1}$	$\mathbf{1}$
$U(1)_X$	$-\frac{1}{3}$	$\frac{2}{3}$	0	0	0	0	0	0	0	0	0	0
D_4	$\mathbf{1}_{+-}$	$\mathbf{1}_{++}$	$\mathbf{2}$	$\mathbf{2}$	$\mathbf{1}_{-+}$	$\mathbf{1}_{++}$	$\mathbf{1}_{--}$	$\mathbf{2}$	$\mathbf{1}_{--}$	$\mathbf{2}$	$\mathbf{1}_{+-}$	$\mathbf{1}_{++}$
Z_4	-1	1	0	2	0	-1	-1	0	1	1	-2	-2
$Z_3^{(1)}$	0	0	0	0	0	-1	-1	0	0	0	0	0
$Z_3^{(2)}$	0	0	0	0	0	0	0	-1	2	2	-2	-2
Z_{16}	0	0	0	0	-1	-1	-1	0	-8	-8	0	0

Table 2 Fermion transformations under the $SU(3)_C \times SU(3)_L \times U(1)_X \times D_4 \times Z_4 \times Z_3^{(1)} \times Z_3^{(2)} \times Z_{16}$ group

	Q_{1L}	Q_{2L}	Q_{3L}	u_{1R}	u_{2R}	u_{3R}	d_{1R}	D_R	J_{1R}	J_{2R}	J_{3R}	L_L	L_{3L}	l_{1R}	l_{2R}	l_{3R}	N_R	N_{3R}	E_L	E_R
$SU(3)_C$	$\mathbf{3}$	$\mathbf{3}$	$\mathbf{3}$	$\mathbf{3}$	$\mathbf{3}$	$\mathbf{3}$	$\mathbf{3}$	$\mathbf{3}$	$\mathbf{3}$	$\mathbf{3}$	$\mathbf{3}$	$\mathbf{1}$	$\mathbf{1}$	$\mathbf{1}$	$\mathbf{1}$	$\mathbf{1}$	$\mathbf{1}$	$\mathbf{1}$	$\mathbf{1}$	$\mathbf{1}$
$SU(3)_L$	$\mathbf{3}$	$\bar{\mathbf{3}}$	$\bar{\mathbf{3}}$	$\mathbf{1}$	$\mathbf{1}$	$\mathbf{1}$	$\mathbf{1}$	$\mathbf{1}$	$\mathbf{1}$	$\mathbf{1}$	$\mathbf{1}$	$\mathbf{3}$	$\mathbf{3}$	$\mathbf{1}$	$\mathbf{1}$	$\mathbf{1}$	$\mathbf{1}$	$\mathbf{1}$	$\mathbf{1}$	$\mathbf{1}$
$U(1)_X$	$\frac{1}{3}$	0	0	$\frac{2}{3}$	$\frac{2}{3}$	$\frac{2}{3}$	$-\frac{1}{3}$	$-\frac{1}{3}$	$\frac{2}{3}$	$-\frac{1}{3}$	$-\frac{1}{3}$	$-\frac{1}{3}$	$-\frac{1}{3}$	-1	-1	-1	0	0	-1	-1
D_4	$\mathbf{1}_{+-}$	$\mathbf{1}_{-+}$	$\mathbf{1}_{--}$	$\mathbf{1}_{-+}$	$\mathbf{1}_{-+}$	$\mathbf{1}_{--}$	$\mathbf{1}_{-+}$	$\mathbf{2}$	$\mathbf{1}_{++}$	$\mathbf{1}_{--}$	$\mathbf{1}_{-+}$	$\mathbf{2}$	$\mathbf{1}_{++}$	$\mathbf{1}_{+-}$	$\mathbf{1}_{--}$	$\mathbf{1}_{-+}$	$\mathbf{2}$	$\mathbf{1}_{+-}$	$\mathbf{2}$	$\mathbf{2}$
Z_4	0	0	2	0	1	-1	-1	0	1	-1	1	0	0	-1	-1	-1	1	1	-1	-1
$Z_3^{(1)}$	-1	0	0	-1	0	0	-1	0	-1	0	0	0	0	0	0	0	0	0	0	0
$Z_3^{(2)}$	0	0	0	0	0	0	0	0	0	0	0	1	1	-1	-1	1	1	1	1	1
Z_{16}	-4	-2	0	3	2	0	0	1	-4	-2	0	-4	-4	0	-4	-1	-4	-4	-4	-4

The scalar and fermionic spectrum and their assignments under the $SU(3)_C \times SU(3)_L \times U(1)_X \times D_4 \times Z_4 \times Z_3^{(1)} \times Z_3^{(2)} \times Z_{16}$ group are shown in Tables 1 and 2, respectively.

With the fermion and scalar contents in Tables 1 and 2, the following quark and lepton Yukawa terms arise:

$$
\begin{aligned}
-\mathcal{L}_Y^{(q)} =\; & y_1^{(J)}\overline{Q}_{1L}\chi J_{1R} + \sum_{n=2}^{3} y_n^{(J)}\overline{Q}_{nL}\chi^* J_{nR} \\
& + y_{33}^{(u)}\overline{Q}_{3L}\rho^* u_{3R} + y_{22}^{(u)}\overline{Q}_{2L}\rho^* u_{2R}\frac{\sigma^4}{\Lambda^4} \\
& + y_{11}^{(u)}\varepsilon_{abc}\overline{Q}_{1L}^a\left(\rho^*\right)^b\left(\chi^*\right)^c u_{1R}\frac{\sigma^7}{\Lambda^7} \\
& + y_{11}^{(d)}\overline{Q}_{1L}\rho d_{1R}\frac{\sigma^4\left(\xi\xi\right)_{\mathbf{1}_{-+}}\left(\xi\xi\right)_{\mathbf{1}_{+-}}}{\Lambda^8} \\
& + y_{12}^{(d)}\overline{Q}_{1L}\rho\left(\xi D_R\right)_{\mathbf{1}_{+-}}\frac{\phi_1\sigma^4}{\Lambda^6} \\
& + y_{13}^{(d)}\overline{Q}_{1L}\rho\left(\xi D_R\right)_{\mathbf{1}_{-+}}\frac{\phi_2\sigma^4}{\Lambda^6} \\
& + y_{22}^{(d)}\varepsilon_{abc}\overline{Q}_{2L}^a\rho^b\chi^c\left(\xi D_R\right)_{\mathbf{1}_{+-}}\frac{\sigma^3}{\Lambda^5} \\
& + y_{33}^{(d)}\varepsilon_{abc}\overline{Q}_{3L}^a\rho^b\chi^c\left(\Xi D_R\right)_{\mathbf{1}_{++}}\frac{\sigma}{\Lambda^3} + H.c, \qquad (5) \\
-\mathcal{L}_Y^{(l)} =\; & y_1^{(l)}\left(\overline{L}_L\rho E_R\right)_{\mathbf{1}_{++}} + z_1^{(l)}\left(\overline{E}_L\Phi\right)_{\mathbf{1}_{+-}} l_{1R}\frac{\sigma^4}{\Lambda^4} \\
& + z_2^{(l)}\left(\overline{E}_L\Phi\right)_{\mathbf{1}_{--}} l_{2R} + m_E\left(\overline{E}_L E_R\right)_{\mathbf{1}_{++}} \\
& + y_3^{(l)}\overline{L}_{3L}\rho l_{3R}\frac{\sigma^3}{\Lambda^3} \\
& + y_{1\chi}^{(L)}\left(\overline{L}_L\chi\right)_{\mathbf{2}} N_R + y_{2\chi}^{(L)}\overline{L}_{3L}\chi N_{3R} \\
& + x_\rho^{(1)}\varepsilon_{abc}\left[\left(\overline{L_L^C}\right)^a\left(L_L\right)^b\right]_{\mathbf{1}_{--}}\left(\rho\right)^c\frac{\zeta^*}{\Lambda} \\
& + x_\rho^{(2)}\varepsilon_{abc}\left[\left(\overline{L_L^C}\right)^a\left(L_{3L}\right)^b\left(\rho\right)^c\right]_{\mathbf{2}}\frac{\eta^*}{\Lambda} \\
& + x_\rho^{(3)}\varepsilon_{abc}\left[\left(\overline{L_{3L}^C}\right)^a\left(L_L\right)^b\left(\rho\right)^c\right]_{\mathbf{2}}\frac{\eta^*}{\Lambda} \\
& + y_{N_1}\left(\overline{N_R^C}N_R\right)_{\mathbf{1}_{+-}}\varphi_1\frac{\sigma^8}{\Lambda^8} \\
& + y_{N_2}\left(\overline{N_R^C}N_R\right)_{\mathbf{1}_{++}}\varphi_2\frac{\sigma^8}{\Lambda^8} \\
& + y_{N_3}\overline{N_{3R}^C}N_{3R}\varphi_2\frac{\sigma^8}{\Lambda^8} + H.c. \qquad (6)
\end{aligned}
$$

The large amount of parametric freedom of the scalar potential allows to consider the following vacuum expectation value (VEV) configuration for the D_4 doublets SM gauge singlet scalars:

$$
\begin{aligned}
& \langle\xi\rangle = \left(v_{\xi_1}, v_{\xi_2}\right) = v_\xi\left(1, r\right), \quad \langle\Xi\rangle = v_\Xi\left(1, 0\right), \\
& \langle\eta\rangle = \left(v_{\eta_1}, v_{\eta_2}\right), \quad \langle\Phi\rangle = \left(v_1, v_2\right), \qquad (7)
\end{aligned}
$$

whereas for the VEVs of the gauge singlet scalars one has:

$$
\langle\sigma\rangle = v_\sigma, \quad \langle\phi_1\rangle = v_{\phi_1}, \quad \langle\phi_2\rangle = v_{\phi_2},
$$

$$\langle \phi \rangle = v_\phi, \quad \langle \zeta \rangle = v_\zeta, \quad \langle \varphi_1 \rangle = v_{\varphi_1}, \quad \langle \varphi_2 \rangle = v_{\varphi_2}. \tag{8}$$

The above given VEV pattern allows to get a predictive and viable pattern of SM fermion masses and mixings as it will be shown in the next sections.

3 Quark masses and mixings

From the quark Yukawa terms given in Eq. (5), it follows that the SM mass matrices for quarks are:

$$M_U = \begin{pmatrix} a_1^{(U)}\lambda^8 & 0 & 0 \\ 0 & a_2^{(U)}\lambda^4 & 0 \\ 0 & 0 & a_3^{(U)} \end{pmatrix},$$

$$M_D = \begin{pmatrix} a_1^{(D)}\lambda^8 & \left(a_4^{(D)} + a_5^{(D)}\right)\lambda^6 & \left(a_4^{(D)} - a_5^{(D)}\right) r\lambda^6 \\ 0 & a_2^{(D)}\lambda^5 & a_{23}^{(D)}\lambda^5 \\ 0 & 0 & a_3^{(D)}\lambda^3 \end{pmatrix}$$

$$= \begin{pmatrix} a_1^{(D)}\lambda^8 & a_{12}^{(D)}\lambda^6 & a_{13}^{(D)}\lambda^6 \\ 0 & a_2^{(D)}\lambda^5 & a_{23}^{(D)}\lambda^5 \\ 0 & 0 & a_3^{(D)}\lambda^3 \end{pmatrix}, \tag{9}$$

where $a_1^{(U)}, a_1^{(D)}, \ldots$ are $\mathcal{O}(1)$ dimensionless parameters which are given by:

$$a_1^{(U)} = \frac{y_{11}^{(u)}}{2} v_\rho, \quad a_2^{(U)} = \frac{y_{22}^{(u)}}{\sqrt{2}} v_\rho, \quad a_3^{(U)} = \frac{y_{33}^{(u)}}{\sqrt{2}} v_\rho,$$
$$a_1^{(D)} = \frac{y_{11}^{(d)}}{\sqrt{2}} v_\rho, \quad a_2^{(D)} = \frac{y_{22}^{(d)}}{2} v_\rho, \quad a_3^{(D)} = \frac{y_{33}^{(d)}}{2} v_\rho,$$
$$a_4^{(D)} = \frac{y_{12}^{(d)}}{\sqrt{2}} v_\rho, \quad a_5^{(D)} = \frac{y_{13}^{(d)}}{\sqrt{2}} v_\rho,$$
$$\frac{v_\Xi}{\Lambda} \sim \frac{v_\xi}{\Lambda} \sim \frac{v_\chi}{\Lambda} \sim \frac{v_{\phi_1}}{\Lambda} \sim \frac{v_{\phi_2}}{\Lambda} \sim \frac{v_\sigma}{\Lambda} = \lambda. \tag{10}$$

Here $v = 246$ GeV is the scale of electroweak symmetry breaking and the Wolfenstein parameter $\lambda = 0.225$ is used for characterization of the hierarchy between the parameters defining quark mass matrix elements in Eq. (9). We find that the experimental values for the physical quark mass spectrum [44,45], mixing angles and CP violating phase [44,45] can be well reproduced for the following benchmark point:

$$a_1^{(U)} \simeq 1.085, \quad a_2^{(U)} \simeq 1.413, \quad a_3^{(U)} \simeq 0.994,$$
$$a_1^{(D)} \simeq 2.329, \quad a_2^{(D)} \simeq 0.554,$$
$$a_3^{(D)} \simeq 1.439, \quad a_{12}^{(D)} \simeq 0.570,$$
$$a_{13}^{(D)} \simeq -(0.123 + 0.438i), \quad a_{23}^{(D)} \simeq 1.152. \tag{11}$$

In addition, Fig. 1 shows the correlation plot between the quark mixing parameter $\sin\theta_{13}$ and the Jarlskog invariant. As indicated by Fig. 1, $\sin\theta_{13}$ is predicted to be in range $0.0033 \lesssim \sin\theta_{13} \lesssim 0.0040$ in the allowed parameter space.

Table 3 Model and experimental values of the quark masses and CKM parameters

Observable	Model value	Experimental value
$m_u[MeV]$	1.24	1.24 ± 0.22
$m_c[GeV]$	0.63	0.63 ± 0.02
$m_t[GeV]$	172.9	172.9 ± 0.4
$m_d[MeV]$	2.59	2.69 ± 0.19
$m_s[MeV]$	57.0	53.5 ± 4.6
$m_b[GeV]$	2.86	2.86 ± 0.03
$\sin\theta_{12}$	0.226	0.22650 ± 0.00048
$\sin\theta_{23}$	0.0405	$0.04053^{+0.00083}_{-0.00061}$
$\sin\theta_{13}$	0.00360	$0.00361^{+0.00009}_{-0.00011}$
J_q	0.0000309	$\left(3.00^{+0.15}_{-0.09}\right) \times 10^{-5}$

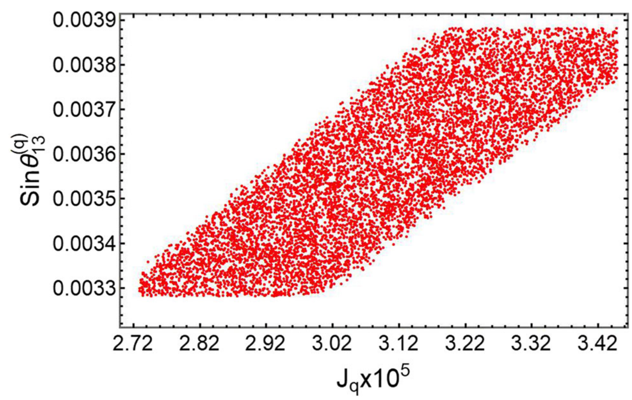

Fig. 1 Correlation plot between the quark mixing parameter $\sin\theta_{13}$ and the Jarlskog invariant

Furthermore, the quark mixing parameter $\sin\theta_{13}$ increases when the Jarlskog invariant takes larger values.

4 Lepton masses and mixings

From the charged-lepton Yukawa interactions in Eq. (6) and the VEV alignments in Eq. (8), we find the following charged -lepton mass terms:

$$-\mathcal{L}_Y^l = (\bar{l}_{1L} \;\; \bar{l}_{2L} \;\; \bar{l}_{3L} \;\; \bar{E}_{1L} \;\; \bar{E}_{2L}) M_l \begin{pmatrix} l_{1R} \\ l_{2R} \\ l_{3R} \\ E_{1R} \\ E_{2R} \end{pmatrix} + \text{H.c}, \tag{12}$$

where the charged-lepton mass matrix is given by

$$M_E = \begin{pmatrix} C_E & A_E \\ B_E & X_E \end{pmatrix}, \quad C_E = \begin{pmatrix} 0 & 0 & 0 \\ 0 & 0 & 0 \\ 0 & 0 & y_3^{(l)} \end{pmatrix} \frac{v_\sigma^3 v_\rho}{\Lambda^3\sqrt{2}}$$

$$= \begin{pmatrix} 0 & 0 & 0 \\ 0 & 0 & 0 \\ 0 & 0 & c \end{pmatrix} \frac{v_\rho}{\sqrt{2}}, \tag{13}$$

$$A_E = y_1^{(l)} \begin{pmatrix} 0 & 1 \\ 1 & 0 \\ 0 & 0 \end{pmatrix} \frac{v_\rho}{\sqrt{2}},$$

$$B_E = \begin{pmatrix} z_1^{(l)} \frac{v_\sigma^2}{\Lambda^2} v_1 & z_2^{(l)} v_2 & 0 \\ z_1^{(l)} \frac{v_\sigma^2}{\Lambda^2} v_2 & -z_2^{(l)} v_1 & 0 \end{pmatrix}$$

$$= \begin{pmatrix} a v_1 & b v_2 & 0 \\ a v_2 & -b v_1 & 0 \end{pmatrix}, \tag{14}$$

$$X_E = \begin{pmatrix} 0 & 1 \\ 1 & 0 \end{pmatrix} m_E,$$

$$a = z_1^{(l)} \frac{v_\sigma^2}{\Lambda^2}, \quad b = z_2^{(l)}, \quad c = y_3^{(l)} \frac{v_\sigma^3}{\Lambda^3}. \tag{15}$$

Then, the SM charged lepton mass matrix takes the form:

$$M_l = C_E + A_E X_E^{-1} B_E = \begin{pmatrix} \alpha v_1 & \beta v_2 & 0 \\ \alpha v_2 & -\beta v_1 & 0 \\ 0 & 0 & c\frac{v_\rho}{\sqrt{2}} \end{pmatrix}$$

$$\equiv \begin{pmatrix} m_{11} & -m_{12} & 0 \\ m_{21} & m_{22} & 0 \\ 0 & 0 & m_{33} \end{pmatrix} \tag{16}$$

Let us define a Hermitian matrix M_l as follows

$$m_l^2 = M_l M_l^+ = \begin{pmatrix} |m_{11}|^2 + |m_{12}|^2 & m_{11}m_{21}^2 - m_{12}m_{22}^* & 0 \\ (m_{11}m_{21}^* - m_{12}m_{22}^*)^* & |m_{21}|^2 + |m_{22}|^2 & 0 \\ 0 & & |m_{33}|^2 \end{pmatrix}, \tag{17}$$

which can be diagonalized by $U_{L,R}$ satisfying $U_L^+ m_l^2 U_R = \mathrm{diag}(m_e^2, m_\mu^2, m_\tau^2)$, where

$$U_L = U_R = \begin{pmatrix} \cos\theta & -\sin\theta.e^{-i\alpha} & 0 \\ \sin\theta.e^{i\alpha} & \cos\theta & \\ 0 & & 1 \end{pmatrix}, \tag{18}$$

$$m_{e,\mu}^2 = \lambda_1 \mp \lambda_2, \quad m_\tau^2 = |m_{33}|^2, \tag{19}$$

with

$$2\lambda_2 = \Big\{ |m_{11}|^4 + (|m_{21}|^2 - |m_{12}|^2)^2 + 2(|m_{21}|^2 + |m_{12}|^2)|m_{22}|^2 + 2|m_{11}|^2(|m_{21}|^2 + |m_{12}|^2 - |m_{22}|^2) + |m_{22}|^4 - 8|m_{11}||m_{21}||m_{12}||m_{22}|\cos(\delta_{12} - \beta_{12}) \Big\}^{\frac{1}{2}},$$

$$\delta_{12} = \alpha_1 - \alpha_2, \beta_{12} = \beta_1 - \beta_2, \tag{20}$$

$$2\lambda_1 = |m_{11}|^2 + |m_{21}|^2 + |m_{12}|^2 + |m_{22}|^2, \quad \alpha_i = \arg(a_i), \quad \beta_i = \arg(b_i) \quad (i = 1, 2), \tag{21}$$

$$\alpha = \frac{i}{2} \log\left(\frac{m_{11}m_{21}^* - m_{12}m_{22}^*}{m_{11}^* m_{21} - m_{12}^* m_{22}} \right),$$

$$\theta = \arctan\left(\frac{(m_{11}^* m_{21} - m_{12}^* m_{22})e^{-i\alpha}}{|m_{11}|^2 + |m_{12}|^2 - m_\mu^2} \right). \tag{22}$$

By comparing the obtained result in Eq. (19) with the experimental values of the charged-lepton masses taken from Ref. [45], $m_e = 0.51099$ MeV, $m_\mu = 105.65837$ MeV, $m_\tau = 1776.86$ MeV, we obtain:

$$|m_{33}| = 1.77686 \times 10^9 \text{ eV}, \lambda_1 = 5.58198 \times 10^{15} \text{ eV}^2, \quad \lambda_2 = 5.58172 \times 10^{15} \text{ eV}^2. \tag{23}$$

In the case $v_1 = v.e^{i\vartheta_1}$, $v_2 = v.e^{i\vartheta_2}$, we get:

$$|m_{11}| = |m_{21}| = 3.61324 \times 10^5 \text{ eV}, \quad |m_{12}| = |m_{22}| = 7.47117 \times 10^7 \text{ eV}. \tag{24}$$

As we will see below, since the charged lepton mixing matrix U_L is non trivial, it can contribute to the leptonic mixing matrix, defined by $U = U_L^+ U_\nu$ where U_ν being neutrino mixing matrix.

Regarding the neutrino sector, from the lepton Yukawa terms in Eq. (6) and the VEV alignments in Eq. (8), we find the following neutrino mass terms:

$$-\mathcal{L}_{mass}^\nu = \frac{1}{2} \left(\overline{\nu_L^C} \; \overline{\nu_R^C} \; \overline{N_R^C} \right) M_\nu \begin{pmatrix} \nu_L \\ \nu_R \\ N_R \end{pmatrix} + H.c, \tag{25}$$

where the neutrino mass matrix reads:

$$M_\nu = \begin{pmatrix} 0_{3\times3} & M_{\nu_D} & 0_{3\times3} \\ M_{\nu_D}^T & 0_{3\times3} & M_\chi \\ 0_{3\times3} & M_\chi^T & M_R \end{pmatrix}, \tag{26}$$

and the submatrices are given by:

$$M_{\nu_D} = \begin{pmatrix} 0 & -a & -b_1 \\ a & 0 & -b_2 \\ b_1 & b_2 & 0 \end{pmatrix} \frac{1}{\Lambda} \frac{v_\rho}{\sqrt{2}}, \quad M_\chi = m_N \begin{pmatrix} 1 & 0 & 0 \\ 0 & 1 & 0 \\ 0 & 0 & x \end{pmatrix},$$

$$M_R = \begin{pmatrix} \kappa_1 & \kappa_2 & 0 \\ \kappa_2 & \kappa_1 & 0 \\ 0 & 0 & \kappa_3 \end{pmatrix} \mu, \tag{27}$$

with

$$a = x_\rho^{(1)} v_\zeta, \quad b_{1,2} = x_\rho^{(2)} v_{\eta_{2,1}} = -x_\rho^{(3)} v_{\eta_{2,1}},$$

$$x = \frac{y_{2\chi}^{(L)}}{y_{1\chi}^{(L)}}, \quad m_N = y_{1\chi}^{(L)} \frac{v_\chi}{\sqrt{2}}, \quad \kappa_1 = y_{1N}, \quad \kappa_2 = y_{2N} \frac{v_{\varphi_2}}{v_{\varphi_1}},$$

$$\kappa_3 = y_{3N} \frac{v_{\varphi_2}}{v_{\varphi_1}}, \quad \mu = \frac{v_{\varphi_1} v_\sigma^8}{\Lambda^8}. \tag{28}$$

It is worth mentioning that the 22 block of the full neutrino mass matrix can be generated from the Feynman diagram of Fig. 2, which involves the virtual exchange of ξ_χ, ζ_χ, Z' as well as the Majorana mass terms in the internal lines of the loop. These Majorana mass terms arise from the non

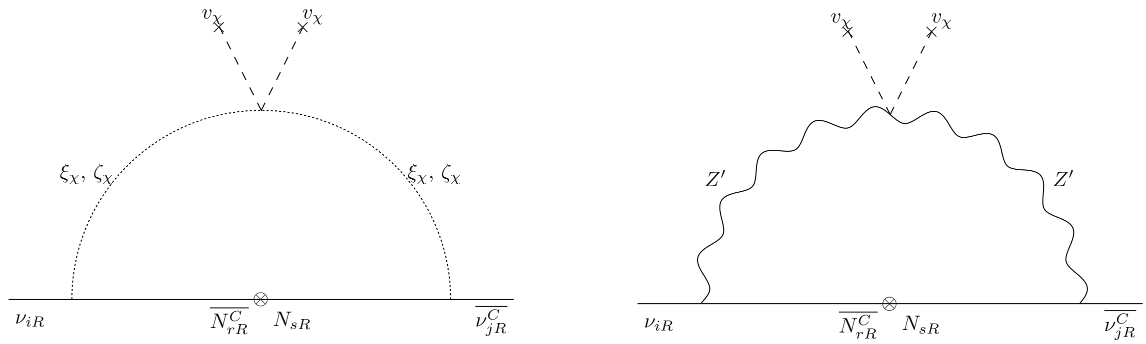

Fig. 2 Feynman diagram contributing to the 22 block of the full neutrino mass matrix. Here, $i, j, r, s = 1, 2, 3$ and the cross mark $\otimes$ in the internal lines corresponds to the Majorana mass terms induced by the dimension twelve Majorana neutrino Yukawa interactions of Eq. (6)

renormalizable Majorana neutrino Yukawa interactions of Eq. (6). Given that the non renormalizable Majorana neutrino Yukawa terms are of dimension 12 as shown in Eq. (6), we have that the entries of the the 22 block of the full neutrino mass matrix are much smaller than the entries of the M_R submatrix and thus they give very subleading corrections to the physical neutrino mass matrices.

The light active masses arise from an inverse seesaw mechanism and the physical neutrino mass matrices are:

$$M_\nu^{(1)} = M_{\nu_D}\left(M_\chi^T\right)^{-1} M_R M_\chi^{-1} M_{\nu_D}^T, \tag{29}$$

$$M_\nu^{(2)} = -\frac{1}{2}\left(M_\chi + M_\chi^T\right) + \frac{1}{2}M_R, \qquad M_\nu^{(3)} = \frac{1}{2}\left(M_\chi + M_\chi^T\right) + \frac{1}{2}M_R, \tag{30}$$

where $M_\nu^{(1)}$ is the light active neutrino mass matrix whereas $M_\nu^{(2)}$ and $M_\nu^{(3)}$ are the exotic Dirac neutrino mass matrices. It is worth mentioning that physical neutrino spectrum consists of three light active neutrinos and six exotic neutrinos. The exotic neutrinos are pseudo-Dirac, with masses $\sim \pm v_\chi \sim \mathcal{O}(10)$ TeV and a small splitting $\sim \mu$.

The mass matrix for light active neutrinos takes the form:

$$M_\nu^{(1)} = \begin{pmatrix} a^2\kappa_1 + \frac{b_1^2\kappa_3}{x^2} & -a^2\kappa_2 + \frac{b_1 b_2\kappa_3}{x^2} & -a(b_2\kappa_1 + b_1\kappa_2) \\ -a^2\kappa_2 + \frac{b_1 b_2\kappa_3}{x^2} & a^2\kappa_1 + \frac{b_2^2\kappa_3}{x^2} & a(b_1\kappa_1 + b_2\kappa_2) \\ -a(b_2\kappa_1 + b_1\kappa_2) & a(b_1\kappa_1 + b_2\kappa_2) & (b_1^2 + b_2^2)\kappa_1 + 2b_1 b_2\kappa_2 \end{pmatrix} m_\nu, \tag{31}$$

where:

$$m_\nu = \frac{v_\rho^2}{2\Lambda^2} m_N^2 \mu. \tag{32}$$

The mass matrix $M_\nu^{(1)}$ has three exact eigenvalues as follows:

$$m_1 = 0, \quad m_{2,3} = \mathbb{k}_1 \mp \mathbb{k}_2, \tag{33}$$

where

$$\begin{aligned} \mathbb{k}_1 &= \frac{m_\nu}{2}\left[2a^2\kappa_1 + (b_1^2 + b_2^2)\kappa_1 + 2b_1 b_2\kappa_2 + \frac{(b_1^2 + b_2^2)\kappa_3}{x^2}\right], \\ \mathbb{k}_2 &= \frac{m_\nu}{2}\frac{\sqrt{\mathbb{k}}}{x^2}, \\ \mathbb{k} &= (b_1^2 + b_2^2)^2\kappa_3^2 - 2\left[(b_1^2 + b_2^2)^2\kappa_1 \right. \\ &\quad \left. + 2b_1 b_2(2a^2 + b_1^2 + b_2^2)\kappa_2\right]\kappa_3 x^2 \end{aligned} \tag{34}$$

$$\begin{aligned} &+ \left[(b_1^2 + b_2^2)^2\kappa_1^2 + 4b_1 b_2(2a^2 + b_1^2 + b_2^2)\kappa_1\kappa_2 \right. \\ &\left. + 4(a^2 + b_1^2)(a^2 + b_2^2)\kappa_2^2\right] x^4, \end{aligned} \tag{35}$$

and the corresponding mixing matrix is:

$$R = \begin{pmatrix} \frac{K_1}{\sqrt{K_1^2+N_1^2+1}} & \frac{K_2}{\sqrt{K_2^2+N_2^2+1}} & \frac{K_3}{\sqrt{K_3^2+N_3^2+1}} \\ \frac{N_1}{\sqrt{K_1^2+N_1^2+1}} & \frac{N_2}{\sqrt{K_2^2+N_2^2+1}} & \frac{N_3}{\sqrt{K_3^2+N_3^2+1}} \\ \frac{1}{\sqrt{K_1^2+N_1^2+1}} & \frac{1}{\sqrt{K_2^2+N_2^2+1}} & \frac{1}{\sqrt{K_3^2+N_3^2+1}} \end{pmatrix} P, \tag{36}$$

where $P = \mathrm{diag}(1,\ 1,\ i)$ and $K_{1,2,3},\ N_{1,2,3}$ are defined as

$$\begin{aligned} &K_1 = \frac{b_2}{a}, \quad N_1 = -\frac{b_2}{a}, \quad K_2 = \kappa_{21} + \kappa_{22}, \\ &K_3 = \kappa_{31} - \kappa_{22}, \quad N_2 = \epsilon_{21} + \epsilon_{22}, \quad N_3 = \epsilon_{31} - \epsilon_{22}, \end{aligned} \tag{37}$$

where

$$\begin{aligned} \kappa_{21} &= \left[2(a^2 + b_1^2)b_2\kappa_2 x^2 + b_1^3(\kappa_1 x^2 - \kappa_3)\right]\kappa_0, \\ \kappa_{22} &= b_1\left[b_2^2(\kappa_1 x^2 - \kappa_3) + \sqrt{\mathbb{k}}\right]\kappa_0, \\ \kappa_{31} &= \kappa_{21} + \left[b_1 b_2^2(\kappa_1 x^2 - \kappa_3)\right]\kappa_0, \quad \epsilon_{21} \\ &= \left[2b_1(a^2 + b_2^2)\kappa_2 x^2 + b_2(b_1^2 + b_2^3)(\kappa_1 x^2 - \kappa_3)\right]\kappa_0, \\ \epsilon_{22} &= b_2\sqrt{\mathbb{k}}\kappa_0, \quad \epsilon_{31} = \left\{\left[b_2(b_1^2 + b_2^2)\right.\right. \\ &\quad \left.\left. \kappa_1 + 2b_1(a^2 + b_2^2)\kappa_2\right] x^2 - b_2(b_1^2 + b_2^2)\kappa_3\right\}\kappa_0, \\ \kappa_0 &= \left[2a(b_1^2 - b_2^2)\kappa_2 x^2\right]^{-1}. \end{aligned} \tag{38}$$

It is easy to check that K_i, N_i $(i = 1, 2, 3)$ satisfy the following relations

$$\begin{aligned} &1 + K_1K_2 + N_1N_2 = 0,\\ &1 + K_1K_3 + N_1N_3 = 0,\ \ 1 + K_2K_3 + N_2N_3 = 0. \end{aligned} \tag{39}$$

The matrix $M_\nu^{(1)}$ is diagonalized as

$$\begin{aligned} &U_\nu^\dagger M_\nu^{(1)} U_\nu\\ &= \begin{cases} \begin{pmatrix} 0 & 0 & 0\\ 0 & m_2 & 0\\ 0 & 0 & m_3 \end{pmatrix},\ U_\nu = \begin{pmatrix} \frac{K_1}{\sqrt{K_1^2+N_1^2+1}} & \frac{K_2}{\sqrt{K_2^2+N_2^2+1}} & \frac{iK_3}{\sqrt{K_3^2+N_3^2+1}}\\ \frac{N_1}{\sqrt{K_1^2+N_1^2+1}} & \frac{N_2}{\sqrt{K_2^2+N_2^2+1}} & \frac{iN_3}{\sqrt{K_3^2+N_3^2+1}}\\ \frac{1}{\sqrt{K_1^2+N_1^2+1}} & \frac{1}{\sqrt{K_2^2+N_2^2+1}} & \frac{i}{\sqrt{K_3^2+N_3^2+1}} \end{pmatrix} & \text{for NH},\\ \begin{pmatrix} m_3 & 0 & 0\\ 0 & m_2 & 0\\ 0 & 0 & 0 \end{pmatrix},\ U_\nu = \begin{pmatrix} \frac{K_3}{\sqrt{K_3^2+N_3^2+1}} & \frac{K_2}{\sqrt{K_2^2+N_2^2+1}} & \frac{iK_1}{\sqrt{K_1^2+N_1^2+1}}\\ \frac{N_3}{\sqrt{K_3^2+N_3^2+1}} & \frac{N_2}{\sqrt{K_2^2+N_2^2+1}} & \frac{iN_1}{\sqrt{K_1^2+N_1^2+1}}\\ \frac{1}{\sqrt{K_3^2+N_3^2+1}} & \frac{1}{\sqrt{K_2^2+N_2^2+1}} & \frac{i}{\sqrt{K_1^2+N_1^2+1}} \end{pmatrix} & \text{for IH}, \end{cases} \end{aligned} \tag{40}$$

where $m_{2,3}$ and $K_{1,2,3}, N_{1,2,3}$ are respectively given in Eqs. (33) and (37).

The final leptonic mixing matrices then read:

$$\begin{aligned} U &= U_L^+ U_\nu\\ &= \begin{cases} \begin{pmatrix} \frac{K_1\cos\theta+N_1\sin\theta.e^{-i\alpha}}{\sqrt{K_1^2+N_1^2+1}} & \frac{K_2\cos\theta+N_2\sin\theta.e^{-i\alpha}}{\sqrt{K_2^2+N_2^2+1}} & \frac{K_3\cos\theta+N_3\sin\theta.e^{-i\alpha}}{\sqrt{K_3^2+N_3^2+1}}\\ \frac{N_1\cos\theta-K_1\sin\theta.e^{i\alpha}}{\sqrt{K_1^2+N_1^2+1}} & \frac{N_2\cos\theta-K_2\sin\theta.e^{i\alpha}}{\sqrt{K_2^2+N_2^2+1}} & \frac{N_3\cos\theta-K_3\sin\theta.e^{i\alpha}}{\sqrt{K_3^2+N_3^2+1}}\\ \frac{1}{\sqrt{K_1^2+N_1^2+1}} & \frac{1}{\sqrt{K_2^2+N_2^2+1}} & \frac{1}{\sqrt{K_3^2+N_3^2+1}} \end{pmatrix}.P & \text{for NH},\\ \begin{pmatrix} \frac{K_3\cos\theta+N_3\sin\theta.e^{-i\alpha}}{\sqrt{K_3^2+N_2^3+1}} & \frac{K_2\cos\theta+N_2\sin\theta.e^{-i\alpha}}{\sqrt{K_2^2+N_2^2+1}} & \frac{K_1\cos\theta+N_1\sin\theta.e^{-i\alpha}}{\sqrt{K_1^2+N_1^2+1}}\\ \frac{N_3\cos\theta-K_3\sin\theta.e^{i\alpha}}{\sqrt{K_3^2+N_3^2+1}} & \frac{N_3\cos\theta-K_2\sin\theta.e^{i\alpha}}{\sqrt{K_2^2+N_2^2+1}} & \frac{N_1\cos\theta-K_1\sin\theta.e^{i\alpha}}{\sqrt{K_1^2+N_1^2+1}}\\ \frac{1}{\sqrt{K_3^2+N_2^3+1}} & \frac{1}{\sqrt{K_2^2+N_2^2+1}} & \frac{1}{\sqrt{K_1^2+N_1^2+1}} \end{pmatrix}.P & \text{for IH}. \end{cases} \end{aligned} \tag{41}$$

In the three neutrino oscillation picture [45], the leptonic mixing angles $\theta_{12}, \theta_{23}, \theta_{13}$ can be defined via the elements of the leptonic mixing matrix as[1]:

$$\begin{aligned} s_{13}^2 &= |U_{13}|^2\\ &= \begin{cases} \frac{K_3^2\cos^2\theta+K_3N_3\cos(2\theta)\cos\alpha+N_3^2\sin^2\theta}{1+K_3^2+N_3^2} \text{for NH},\\ \frac{K_1^2\cos^2\theta+K_1N_1\sin(2\theta)\cos\alpha+N_1^2\sin^2\theta}{1+K_1^2+N_1^2} \text{for IH}, \end{cases}\\ t_{12}^2 &= \left|\frac{U_{12}}{U_{11}}\right|^2\\ &= \begin{cases} \frac{(1+K_1^2+N_1^2)(K_2^2\cos^2\theta+K_2N_2\sin(2\theta)\sin\alpha+N_2^2\sin^2\theta)}{(1+K_2^2+N_2^2)(K_1^2\cos^2\theta+K_1N_1\sin(2\theta)\sin\alpha+N_1^2\sin^2\theta)} & \text{for NH},\\ \frac{(1+K_3^2+N_3^2)(K_2^2\cos^2\theta+K_2N_2\sin(2\theta)\cos\alpha+N_2^2\sin^2\theta)}{(1+K_2^2+N_2^2)(K_3^2\cos^2\theta+K_3N_3\sin(2\theta)\cos\alpha+N_3^2\sin^2\theta)} & \text{for IH}, \end{cases}\\ t_{23}^2 &= \left|\frac{U_{23}}{U_{33}}\right|^2\\ &= \begin{cases} N_3^2\cos^2\theta - K_3N_3\sin(2\theta)\cos\alpha + K_3^2\sin^2\theta & \text{for NH},\\ N_1^2\cos^2\theta - K_1N_1\sin(2\theta)\cos\alpha + K_1^2\sin^2\theta & \text{for IH}. \end{cases} \end{aligned} \tag{42}$$

[1] Here, $c_{ij} = \cos\theta_{ij}$, $s_{ij} = \sin\theta_{ij}$ with θ_{12} , θ_{23} and θ_{13} being the solar, atmospheric and reactor angle, respectively.

In fact, the neutrino mass spectrum is currently unknown and it can have a normal or inverted ordering depending on the sign of Δm_{31}^2 (or Δm_{32}^2) [45]. As will see below, the lepton mixing matrices in Eq. (54) and neutrino masses in Eq. (33) can fit the observed neutrino mass and mixing pattern taken from Ref. [46] for both Normal and Inverted hierarchies.

The Jarlskog invariant J_{CP} associated with the Dirac phase δ_{CP}, which controls the magnitude of CP violation effects in neutrino oscillations [45], is given by:

$$\begin{aligned} J_{CP} &= \mathrm{Im}(U_{23}U_{13}^*U_{12}U_{22}^*)\\ &= \begin{cases} \frac{(K_2N_3-K_3N_2)(K_2K_3+N_2N_3)}{(1+K_2^2+N_2^2)(1+K_3^2+N_3^2)}\sin\theta\cos\theta\sin\alpha \text{for NH},\\ \frac{(K_2N_1-K_1N_2)(K_1K_2+N_1N_2)}{(1+K_1^2+N_1^2)(1+K_2^2+N_2^2)}\sin\theta\cos\theta\sin\alpha \text{for IH}. \end{cases} \end{aligned} \tag{43}$$

where Eqs. (39) and (41) were taken into account.

By comparing Eq. (43) with its corresponding expression taken from Ref. [45], $J_{CP} = s_{13}c_{13}^2s_{12}c_{12}s_{23}c_{23}\sin\delta$, we get:

$$\sin\delta = \begin{cases} \frac{(K_2N_3-K_3N_2)(K_2K_3+N_2N_3)}{(1+K_2^2+N_2^2)(1+K_3^2+N_3^2)}\frac{\sin\theta\cos\theta\sin\alpha}{s_{13}c_{13}^2s_{12}c_{12}s_{23}c_{23}} \text{for NH},\\ \frac{(K_2N_1-K_1N_2)(K_1K_2+N_1N_2)}{(1+K_1^2+N_1^2)(1+K_2^2+N_2^2)}\frac{\sin\theta\cos\theta\sin\alpha}{s_{13}c_{13}^2s_{12}c_{12}s_{23}c_{23}} \text{for IH}. \end{cases} \tag{44}$$

Combining Eqs. (39), (41) and (42), we found that N_i, K_i $(i = 1, 2, 3)$ and all the elements of leptonic mixing matrix U depend on five parameters $\theta_{12}, \theta_{13}, \theta_{23}, \theta$ and α. By using the best-fit values of leptonic mixing angles taken from Ref. [46],

$$\begin{aligned} &\sin^2\theta_{12} = 0.304,\ \ \sin^2\theta_{23} = \begin{cases} 0.573 & \text{for NH},\\ 0.575 & \text{for IH}, \end{cases}\\ &\sin^2\theta_{13} = \begin{cases} 0.02219 & \text{for NH},\\ 0.02238 & \text{for IH}, \end{cases} \end{aligned} \tag{45}$$

we find out the regions of θ and α which can reproduce the recent experimental data. Indeed, in the case where $\sin\theta = 0.25\,(\theta = 14.5^\circ)$, N_i and K_i depend on α with $\sin\alpha \in (0.40, 0.50)$ for NH and $\sin\alpha \in (0.65, 0.75)$ for IH which is plotted in Fig. 3.

Next, taking the best-fit values of the solar and atmospheric neutrino squared-mass differences taken form Ref. [46],

$$\begin{aligned} \Delta m_{21}^2 &= 7.42\times10^{-5}\,\mathrm{eV}^2,\\ &\times\begin{cases} \Delta m_{31}^2 = 2.517\times10^{-3}\,\mathrm{eV}^2 & \text{for NH},\\ \Delta m_{32}^2 = -2.498\times10^{-3}\,\mathrm{eV}^2 & \text{for IH}, \end{cases} \end{aligned} \tag{46}$$

we get a solution

$$\Bbbk_1 = \begin{cases} 2.94\times10^{-2}\,\mathrm{eV} & \text{for NH},\\ 4.96\times10^{-2}\,\mathrm{eV} & \text{for IH}, \end{cases}$$

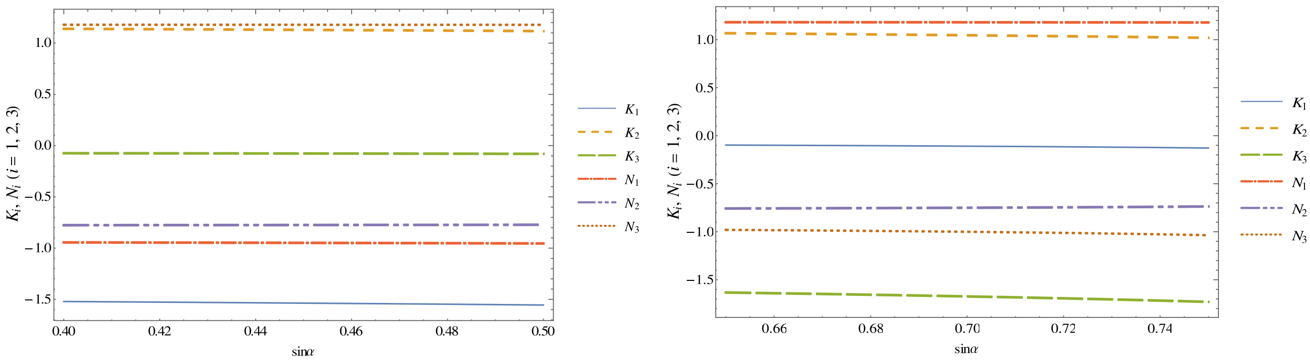

Fig. 3 K_i, N_i versus $\sin\alpha$ with $\sin\alpha \in (0.40, 0.50)$ for NH (left figure) and $\sin\alpha \in (0.65, 0.75)$ for IH (right figure)

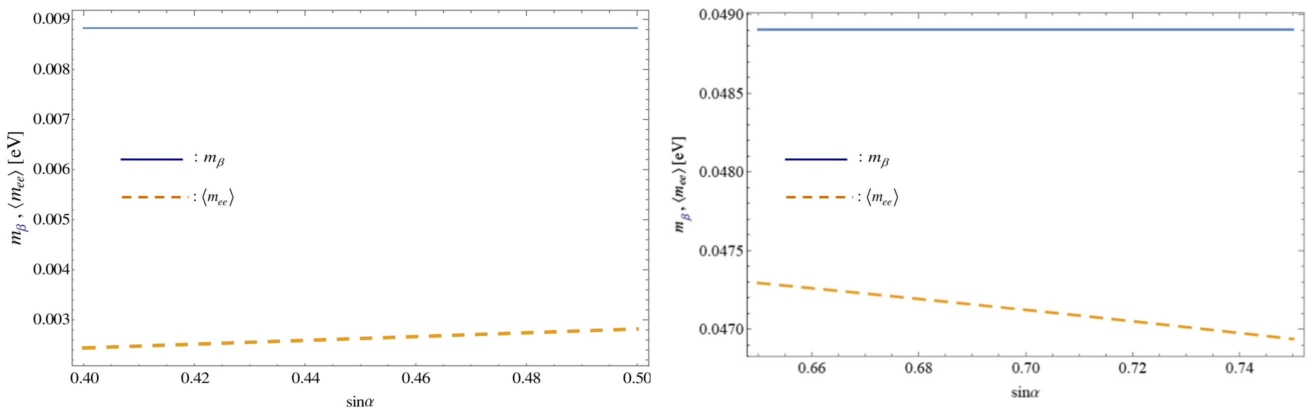

Fig. 4 $\langle m_{ee}\rangle$ and m_β versus $\sin\alpha$ with $\sin\alpha \in (0.40, 0.50)$ for NH (left figure) and $\sin\alpha \in (0.65, 0.75)$ for IH (right figure)

$$\Bbbk_2 = \begin{cases} 2.08 \times 10^{-2}\,\text{eV} & \text{for NH,} \\ -3.74 \times 10^{-4}\,\text{eV} & \text{for IH,} \end{cases} \tag{47}$$

and three neutrino masses are explicitly given as

$$m_1 = 0\,\text{eV}, \quad m_2 = 8.61 \times 10^{-3}\,\text{eV},$$
$$m_3 = 5.02 \times 10^{-2}\,\text{eV} \quad \text{for NH,} \tag{48}$$
$$m_1 = 4.92 \times 10^{-2}\,\text{eV}, \quad m_2 = 5.0 \times 10^{-2}\,\text{eV},$$
$$m_3 = 0\,\text{eV} \quad \text{for IH.} \tag{49}$$

The sum of three neutrino masses is thus found to be

$$\sum_{i=1}^{3} m_i = \begin{cases} 5.88 \times 10^{-2}\,\text{eV} & \text{for NH,} \\ 9.92 \times 10^{-2}\,\text{eV} & \text{for IH,} \end{cases} \tag{50}$$

which are well consistent with the updated bounds from cosmology [47].

Furthermore, in the NH, $m_1 \approx m_2 < m_3$, so $m_1 = 0$ is the lightest neutrino mass while $m_3 = 0$ is the lightest neutrino mass for IH. The effective neutrino mass parameters governing the beta decay and neutrinoless double beta decay, $m_\beta = \sqrt{\sum_{i=1}^{3} |U_{1i}|^2\, m_i^2}$ and $\langle m_{ee}\rangle = \left|\sum_{i=1}^{3} U_{1i}^2 m_i\right|$ depend only on $\sin\alpha$ with $\sin\alpha \in (0.40, 0.50)$ for NH and $\sin\alpha \in (0.65, 0.75)$ for IH which is depicted in Fig. 4.

In the case where $\sin\alpha = 0.445$ ($\alpha = 26.4^\circ$) for NH and $\sin\alpha = 0.75$ ($\alpha = 48.6^\circ$) for IH, m_β and $\langle m_{ee}\rangle$ are found to be:

$$\langle m_{ee}\rangle = \begin{cases} 2.61 \times 10^{-3}\,\text{eV} & \text{for NH,} \\ 4.69 \times 10^{-2}\,\text{eV} & \text{for IH,} \end{cases} \tag{51}$$

and

$$m_\beta = \begin{cases} 8.83 \times 10^{-3}\,\text{eV} & \text{for NH,} \\ 4.89 \times 10^{-2}\,\text{eV} & \text{for IH.} \end{cases} \tag{52}$$

The Jarlskog invariant J_{CP}, determined from Eq. (43), possessed the following values:

$$J_{CP} = \begin{cases} -0.0199 & \text{for NH,} \\ -0.0323 & \text{for IH.} \end{cases} \tag{53}$$

The lepton mixing matrices for both normal and inverted hierarchies take the explicit forms

$$U = \begin{cases} \begin{pmatrix} -0.823 + 0.0511i & 0.543 + 0.0508i & 0.0847 + 0.123i \\ -0.279 + 0.0828i & -0.591 - 0.0741i & -0.0051 + 0.749i \\ 0.481 & 0.589 & 0.646i \end{pmatrix} & \text{for NH,} \\ \begin{pmatrix} -0.82 + 0.0863i & 0.538 + 0.086i & 0.143 + 0.0455i \\ -0.319 + 0.144i & -0.549 - 0.119i & -0.0155 + 0.75i \\ 0.444 & 0.622 & 0.645i \end{pmatrix} & \text{for IH,} \end{cases} \tag{54}$$

Table 4 The model parameters in the case $\sin\theta = 0.25$, and $\sin\alpha = 0.445$ for NH and $\sin\theta = 0.25$ and $\sin\alpha = 0.75$ for IH

Parameters	The derived values (NH)	The derived values (IH)
K_1	-1.53	-0.128
K_2	1.13	1.02
K_3	-0.0767	-1.73
N_1	-0.948	1.18
N_2	-0.775	-0.737
N_3	1.18	-1.04

which are unitary and consistent with the constraint on the absolute values of the entries of the lepton mixing matrix given in Ref. [46]. The other model parameters are obtained as in Table 4.

5 Scalar potential with two $SU(3)_L$ triplets

To simplify our analysis, we neglect the mixing terms between the $SU(3)_L$ scalar triplets and the gauge singlet scalars. Then, the scalar potential for the two $SU(3)_L$ scalar triplets is given by:

$$
\begin{aligned}
V = &-\mu_\chi^2(\chi^\dagger\chi) - \mu_\rho^2(\rho^\dagger\rho) + \lambda_1(\chi^\dagger\chi)(\chi^\dagger\chi)\\
&+\lambda_2(\rho^\dagger\rho)(\rho^\dagger\rho)\\
&+\lambda_3(\chi^\dagger\chi)(\rho^\dagger\rho) + \lambda_4(\chi^\dagger\rho)(\rho^\dagger\chi) + H.c.,
\end{aligned}
$$

with χ and ρ, the $SU(3)_L$ scalar triplets. Furthermore, the global minimum conditions of the scalar potential give the relations:

$$\mu_\chi^2 = \frac{1}{2}\left(2v_\chi^2\lambda_1 + v_\rho^2\lambda_3\right), \tag{55}$$

$$\mu_\rho^2 = \frac{1}{2}\left(2v_\rho^2\lambda_2 + v_\chi^2\lambda_3\right). \tag{56}$$

After spontaneous symmetry breaking we get the squared mass matrices for the scalar fields:

$$
\begin{aligned}
M^2_{CPeven} &= \begin{pmatrix} 0 & 0 & 0 \\ 0 & v_\rho^2\lambda_2 & \frac{1}{2}v_\rho v_\chi\lambda_3 \\ 0 & \frac{1}{2}v_\rho v_\chi\lambda_3 & v_\chi^2\lambda_1 \end{pmatrix},\\
M^2_{CPodd} &= \begin{pmatrix} 0 & 0 & 0 \\ 0 & 0 & 0 \\ 0 & 0 & 0 \end{pmatrix},\\
M^2_{charged} &= \begin{pmatrix} 0 & 0 & 0 \\ 0 & \frac{1}{2}v_\rho^2\lambda_4 & \frac{1}{2}v_\rho v_\chi\lambda_4 \\ 0 & \frac{1}{2}v_\rho v_\chi\lambda_4 & \frac{1}{2}v_\chi^2\lambda_4 \end{pmatrix}.
\end{aligned} \tag{57}
$$

This shows that the resulting physical scalar spectrum arising from the $SU(3)_L$ scalar triplets χ and ρ is composed of the 126 GeV SM like Higgs boson, a heavy neutral CP even scalar H^0 associated with the spontaneous breaking of the $SU(3)_L \times U(1)_X$ symmetry and the electrically charged scalars $H^\pm$. The massless degrees of freedom in the scalar spectrum correspond to the Goldstone boson associated with the longitudinal components of the $W^\pm$, Z, $W'^\pm$, Z', K^0 and $\bar{K}^0$ massive gauge bosons.

6 Higgs diphoton decay rate constraints

The decay rate for the $h \to \gamma\gamma$ process takes the form [48–54]:

$$
\Gamma(h \to \gamma\gamma) = \frac{\alpha_{em}^2 m_h^3}{256\pi^3 v^2}
\left|\sum_f a_{hff} N_C Q_f^2 F_{1/2}(\rho_f) + a_{hWW} F_1(\rho_W) + \frac{C_{hH^\pm H^\mp}}{2m_{H^\pm}^2} v F_0(\rho_{H^\pm})\right|^2, \tag{58}
$$

where ρ_i are the mass ratios $\rho_i = \frac{m_h^2}{4M_i^2}$ with $M_i = m_f, M_W$; α_{em} is the fine structure constant; N_C is the color factor ($N_C = 1$ for leptons and $N_C = 3$ for quarks) and Q_f is the electric charge of the fermion in the loop. From the fermion-loop contributions we only consider the dominant top quark term. Furthermore, $C_{hH^\pm H^\mp}$ is the trilinear coupling between the SM-like Higgs and a pair of charged Higgs bosons, whereas a_{htt} and a_{hWW} are the deviation factors from the SM Higgs top quark coupling and the SM Higgs-W gauge boson coupling, respectively (in the SM these factors are unity). Such deviation factors are very close to unity in our model, which is a consequence of the numerical analysis of its scalar, Yukawa and gauge sectors. Besides, $F_{1/2}(z)$ and $F_1(z)$ are the dimensionless loop factors for spin-1/2 and spin-1 particles running in the internal lines of the loops. They are given by:

$$F_{1/2}(z) = 2(z + (z-1)f(z))z^{-2}, \tag{59}$$

$$F_1(z) = -2(2z^2 + 3z + 3(2z-1)f(z))z^{-2}, \tag{60}$$

$$F_0(z) = -(z - f(z))z^{-2}, \tag{61}$$

with

$$
f(z) = \begin{cases} \left(\arcsin\sqrt{2}\right)^2 & \text{for } z \le 1, \\ -\frac{1}{4}\left(\ln\left(\frac{1+\sqrt{1-z^{-1}}}{1-\sqrt{1-z^{-1}}-i\pi}\right)^2\right) & \text{for } z > 1. \end{cases} \tag{62}
$$

In order to study the implications of our model in the decay of the 126 GeV Higgs boson into a photon pair, one introduces the Higgs diphoton signal strength $R_{\gamma\gamma}$, which is

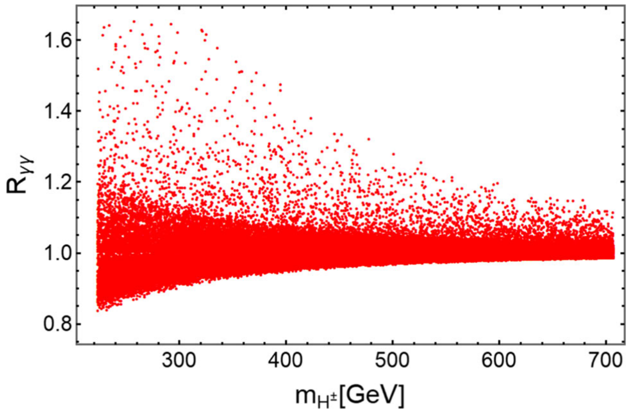

Fig. 5 Higgs diphoton signal strength as a function of the charged scalar mass $m_{H^\pm}$, with $600\,[GeV] < m_{H^\pm} < 7000\,[GeV]$

defined as:

$$R_{\gamma\gamma} = \frac{\sigma(pp \to h)\Gamma(h \to \gamma\gamma)}{\sigma(pp \to h)_{SM}\Gamma(h \to \gamma\gamma)_{SM}} \simeq a_{htt}^2 \frac{\Gamma(h \to \gamma\gamma)}{\Gamma(h \to \gamma\gamma)_{SM}}. \tag{63}$$

That Higgs diphoton signal strength, normalizes the $\gamma\gamma$ signal predicted by our model in relation to the one given by the SM. Here we have used the fact that in our model, single Higgs production is also dominated by gluon fusion as in the Standard Model.

The ratio $R_{\gamma\gamma}$ has been measured by CMS and ATLAS collaborations with the best fit signals [55,56]:

$$R_{\gamma\gamma}^{CMS} = 1.18^{+0.17}_{-0.14} \quad \text{and} \quad R_{\gamma\gamma}^{ATLAS} = 0.96 \pm 0.14. \tag{64}$$

The Higgs diphoton signal strength as a function of the electrically charged scalar mass is shown in Fig. 5. This shows that our model successfully accommodates the current Higgs diphoton decay rate constraints.

7 Muon anomalous magnetic moment

In this section we discuss the implications of our model in the muon anomalous magnetic moment. It is worth mentioning that the dominant contribution to the muon anomalous magnetic moment arises from the one-loop diagram involving the exchange of the electrically neutral scalars h and H and the charged exotic vector like leptons E_1 and E_2. It is worth mentioning that there other contributions to the muon anomalous magnetic moments like the ones arising from the virtual exchange of heavy neutral and electrically charged gauge bosons together with charged and neutral leptons, respectively as well as contributions due to electrically charged scalars and neutrinos. However those extra contributions are subleading. Regarding the contribution arising from the virtual exchange electrically charged scalars and light active neutrinos, we have numerically checked that it can reproduce the magnitude of the $g-2$ muon anomaly for electrically charged scalars lower than 400 GeV. However such contribution turn out to be negative and thus not allow to reproduce the correct sign of the $g-2$ muon anomaly. Consequently, in our analysis of the muon anomalous magnetic moment, we only consider the leading contribution arising from the virtual exchange of electrically neutral scalars h and H and the charged exotic vector like leptons E_1 and E_2. Furthermore, in order to simplify our numerical analysis, we restrict to the region of parameter space where the electrically charged scalars are heavier than about 400 GeV, thus implying that the contribution to the $g-2$ muon anomaly arising from the virtual exchange electrically charged scalars and light active neutrinos is suppressed and therefore subleading. The Feynman diagrams corresponding the Beyond Standard Model contributions to the muon anomalous magnetic moment in the 3-3-1 model under consideration are shown in Fig. 6.

In view of the previous discussion, the dominant contribution to the muon anomalous magnetic moment in our model has the form:

$$\Delta a_\mu \simeq \frac{y_1^{(l)} z_2^{(l)} m_\mu^2}{8\pi^2}\left[J\left(m_{E_2}, m_h\right) - J\left(m_{E_2}, m_H\right)\right] \sin\theta\cos\theta, \tag{65}$$

where, $y_1^{(l)}$ and $z_2^{(l)}$ are the leptonic Yukawa couplings appearing in the first line of Eq. (6). Here, in order to simplify our analysis we have restricted to the case $v_1 \ll v_2$, which implies that only ϕ_1 (the first component of the D_4 scalar doublet Φ) mixes with the CP even neutral part of the $SU(3)_L$ scalar triplet ρ. Then, the neutral scalars h and H are defined as: $H \simeq \cos\theta\,\mathrm{Re}\,\phi_1 + \sin\theta\xi_\rho$, $h \simeq -\sin\theta\,\mathrm{Re}\,\phi_1 + \cos\theta\xi_\rho$, and m_{E_2} is the mass of the VLL E_2. Furthermore, the loop $J(m_E, m_S)$ function has the following form [57–60]:

$$J(m_E, m_S) = \int_0^1 dx \frac{x^2\left(1 - x + \frac{m_E}{m_\mu}\right)}{m_\mu^2 x^2 + \left(m_E^2 - m_\mu^2\right)x + m_S^2(1-x)}. \tag{66}$$

The above given expression for the muon anomalous magnetic moment can be approximately rewritten as follows:

$$\Delta a_\mu \simeq \frac{y_1^{(l)} z_2^{(l)}}{8\pi^2}\left[\frac{m_\mu m_{E_2}}{m_h^2} G_1\left(\frac{m_{E_2}^2}{m_h^2}\right) - \frac{m_\mu m_{E_2}}{m_H^2} G\left(\frac{m_{E_2}^2}{m_H^2}\right)\right] \sin\theta\cos\theta, \tag{67}$$

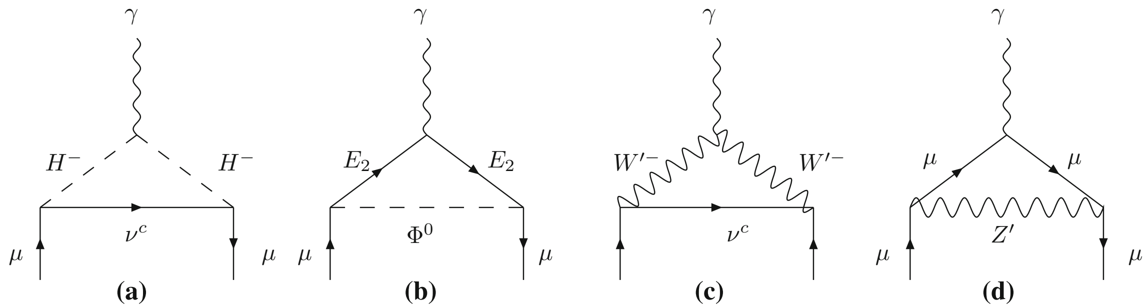

Fig. 6 Feynman diagrams corresponding to Beyond Standard Model contributions to the muon anomalous magnetic moment in the 3-3-1 model under consideration. Notice that the second diagram involving the virtual exchange of charged exotic leptons $E_{1,2}$ and neutral scalars $\Phi^0 = h, H$ is the one that provides the leading contribution to the muon anomalous magnetic moment

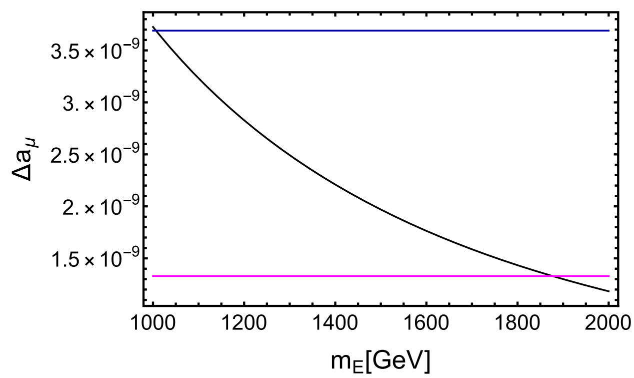

Fig. 7 Muon anomalous magnetic moment as a function of the charged exotic lepton mass m_E

where the corresponding loop function as the form [61]:

$$G(z) = \frac{3 - 4z + z^2 + 2\ln z}{2(z-1)^3}. \tag{68}$$

Considering that the muon anomalous magnetic moment is constrained to be in the range [62–69]

$$\left(\Delta a_\mu\right)_{\exp} = a_\mu^{\exp} - a_\mu^{\mathrm{SM}} = (2.51 \pm 0.59) \times 10^{-9}. \tag{69}$$

We display in Fig. 7 the muon anomalous magnetic moment as a function of the charged exotic vector like mass. As shown in Fig. 7, we have that our model successfully accommodates the experimental value of Δa_μ for charged exotic lepton masses at the TeV scale.

8 Meson oscillations

The non universal $U(1)_X$ charge assignments for the left handed quark fields yield tree level Z' mediated flavour changing neutral processes (FCNC) which will yield $K^0 - \bar{K}^0$, $B_d^0 - \bar{B}_d^0$ and $B_s^0 - \bar{B}_s^0$ meson oscillations. These meson mixings are described by the following effective Hamiltonian interactions [70]:

$$\mathcal{H}_{eff}^{(K^0-\bar{K}^0)} = \frac{4\sqrt{2}G_F c_W^4 m_Z^2}{\left(3-4s_W^2\right)m_{Z'}^2}\left|\left(V_{DL}^*\right)_{32}\left(V_{DL}\right)_{31}\right|^2 O^{(K^0-\bar{K}^0)}, \tag{70}$$

$$\mathcal{H}_{eff}^{(B_d^0-\bar{B}_d^0)} = \frac{4\sqrt{2}G_F c_W^4 m_Z^2}{\left(3-4s_W^2\right)m_{Z'}^2}\left|\left(V_{DL}^*\right)_{31}\left(V_{DL}\right)_{33}\right|^2 O^{(B_d^0-\bar{B}_d^0)}, \tag{71}$$

$$\mathcal{H}_{eff}^{(B_s^0-\bar{B}_s^0)} = \frac{4\sqrt{2}G_F c_W^4 m_Z^2}{\left(3-4s_W^2\right)m_{Z'}^2}\left|\left(V_{DL}^*\right)_{32}\left(V_{DL}\right)_{33}\right|^2 O^{(B_s^0-\bar{B}_s^0)}. \tag{72}$$

where the corresponding operators are given by:

$$O^{(K^0-\bar{K}^0)} = \left(\bar{s}\gamma_\mu P_L d\right)\left(\bar{s}\gamma^\mu P_L d\right),$$

$$O^{(B_d^0-\bar{B}_d^0)} = \left(\bar{d}\gamma_\mu P_L b\right)\left(\bar{d}\gamma^\mu P_L b\right), \tag{73}$$

$$O^{(B_s^0-\bar{B}_s^0)} = \left(\bar{s}\gamma_\mu P_L b\right)\left(\bar{s}\gamma^\mu P_L b\right). \tag{74}$$

Furthermore, the following relations have been taken into account:

$$\begin{aligned}
\widetilde{M}_f &= \left(M_f\right)_{diag} = V_{fL}^\dagger M_f V_{fR},\\
f_{(L,R)} &= V_{f(L,R)}\widetilde{f}_{(L,R)},\\
\overline{f}_{iL}\left(M_f\right)_{ij} f_{jR} &= \overline{\widetilde{f}}_{kL}\left(V_{fL}^\dagger\right)_{ki}\left(M_f\right)_{ij}\left(V_{fR}\right)_{jl}\\
\widetilde{f}_{lR} &= \overline{\widetilde{f}}_{kL}\left(V_{fL}^\dagger M_f V_{fR}\right)_{kl}\widetilde{f}_{lR}\\
&= \overline{\widetilde{f}}_{kL}\left(\widetilde{M}_f\right)_{kl}\widetilde{f}_{lR}\\
&= m_{fk}\overline{\widetilde{f}}_{kL}\widetilde{f}_{kR},\ k = 1, 2, 3.
\end{aligned} \tag{75}$$

Here, $\widetilde{f}_{k(L,R)}$ and $f_{k(L,R)}$ ($k = 1, 2, 3$) are the SM fermionic fields in the mass and interaction bases, respectively.

On the other hand, the $K - \bar{K}$, $B_d^0 - \bar{B}_d^0$ and $B_s^0 - \bar{B}_s^0$ mass splittings are given by:

$$\Delta m_K = \left(\Delta m_K\right)_{SM} + \Delta m_K^{(NP)},$$

$$\Delta m_{B_d} = \left(\Delta m_{B_d}\right)_{SM} + \Delta m_{B_d}^{(NP)},$$

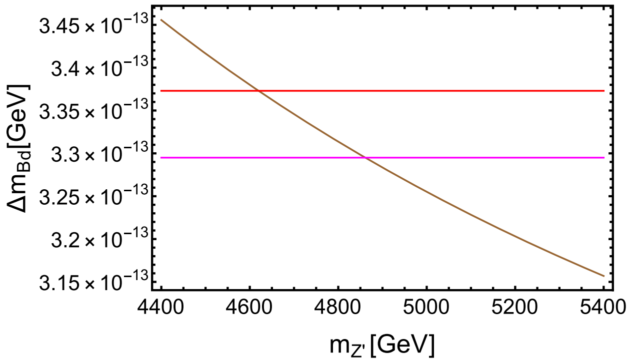

Fig. 8 The $B_d^0-\bar{B}_d^0$ mass splitting as a function of the Z' mass

$$\Delta m_{B_s} = \left(\Delta m_{B_s}\right)_{SM} + \Delta m_{B_s}^{(NP)}, \tag{76}$$

where $(\Delta m_K)_{SM}$, $\left(\Delta m_{B_d}\right)_{SM}$ and $\left(\Delta m_{B_s}\right)_{SM}$ are the SM contributions, whereas $\Delta m_K^{(NP)}$, $\Delta m_{B_d}^{(NP)}$ and $\left(\Delta m_{B_s}\right)_{SM}$ are new physics contributions.

The new physics contributions to meson mass differences are [70]:

$$\Delta m_K^{(NP)} = \frac{4\sqrt{2}G_F c_W^4 m_Z^2}{\left(3-4s_W^2\right)m_{Z'}^2}\left|\left(V_{DL}^*\right)_{32}\left(V_{DL}\right)_{31}\right|^2 f_K^2 B_K \eta_K m_K, \tag{77}$$

$$\Delta m_{B_d}^{(NP)} = \frac{4\sqrt{2}G_F c_W^4 m_Z^2}{\left(3-4s_W^2\right)m_{Z'}^2}\left|\left(V_{DL}^*\right)_{31}\left(V_{DL}\right)_{33}\right|^2 f_{B_d}^2 B_{B_d} \eta_{B_d} m_{B_d}, \tag{78}$$

$$\Delta m_{B_s}^{(NP)} = \frac{4\sqrt{2}G_F c_W^4 m_Z^2}{\left(3-4s_W^2\right)m_{Z'}^2}\left|\left(V_{DL}^*\right)_{32}\left(V_{DL}\right)_{33}\right|^2 f_{B_s}^2 B_{B_s} \eta_{B_s} m_{B_s}. \tag{79}$$

Using the following parameters [70–76]:

$$\begin{aligned}
\Delta m_K &= (3.484 \pm 0.006) \times 10^{-12}\, MeV,\\
(\Delta m_K)_{SM} &= 3.483 \times 10^{-12}\, MeV\\
f_K &= 160\, MeV, \quad B_K = 0.85,\\
\eta_K &= 0.57, \quad m_K = 497.614\, MeV.\\
\left(\Delta m_{B_d}\right)_{\text{exp}} &= (3.337 \pm 0.033) \times 10^{-10}\, MeV,\\
\left(\Delta m_{B_d}\right)_{SM} &= 3.582 \times 10^{-10}\, MeV,\\
f_{B_d} &= 188\, MeV, \quad B_{B_d} = 1.26, \quad \eta_{B_d} = 0.55,\\
m_{B_d} &= 5279.5\, MeV.\\
\left(\Delta m_{B_s}\right)_{\text{exp}} &= (104.19 \pm 0.8) \times 10^{-10}\, MeV,\\
\left(\Delta m_{B_s}\right)_{SM} &= 121.103 \times 10^{-10}\, MeV,\\
f_{B_s} &= 225\, MeV, \quad B_{B_s} = 1.26, \quad \eta_{B_s} = 0.55,\\
m_{B_s} &= 5366.3\, MeV.
\end{aligned}$$

We plot in Fig. 8 the $B_d^0-\bar{B}_d^0$ mass splitting as as function of the Z' mass. As seen from Fig. 8, the obtained values for the $B_s^0-\bar{B}_s^0$ mass difference are consistent with the experimental data where the Z' mass is larger than about 4.6 TeV and lower than about 4.9 TeV. Regarding the $K^0-\bar{K}^0$, $B_d^0-\bar{B}_d^0$ mass splittings, we have numerically checked that the obtained values are in accordance with the meson oscillation experimental data in the above described region of parameter space.

9 Conclusions

We have constructed a theory based on the $SU(3)_C \times SU(3)_L \times U(1)_X$ gauge symmetry, where the scalar sector is composed of two $SU(3)_L$ scalar triplets and several gauge singlet scalar fields. The theory incorporates the D_4 family symmetry, which is supplemented by several auxiliary cyclic symmetries, whose spontaneous breaking yield viable and predictive fermion mass matrix textures with hierarchical entries thus allowing a natural explanation of the current hierarchy of SM fermion masses and mixings. The tiny masses of the light active neutrinos are produced by an inverse seesaw mechanism mediated by three right handed Majorana neutrinos. The smallness of the μ parameter of the inverse seesaw, generated after the spontaneous breaking of the discrete symmetries of the model, is attributed to a right-handed neutrino nonrenormalizable Yukawa terms. Our proposed model is consistent with Higgs diphoton decay rate constraints,with the muon anomalous magnetic moment and the meson oscillation experimental data. The consistency of our model with the muon anomalous magnetic moment requires charged exotic vector like leptons at the TeV scale.

Acknowledgements This research has received funding from ANID-Chile FONDECYT 1210378, ANID PIA/APOYO AFB180002 and ANID-Programa Milenio–code ICN2019_044. H. N. Long acknowledges the financial support of the International Centre of Physics at the Institute of Physics, VAST under Grant No: ICP.2022.02.

Data Availability Statement This manuscript has no associated data or the data will not be deposited. [Authors' comment: This article is based on research in theoretical physics. Therefore, there are no associated data to be deposited.].

Appendix A: The product rules for D_4

The D_4 group has four singlets and one doublet, $\mathbf{1}_{++}$, $\mathbf{1}_{+-}$, $\mathbf{1}_{-+}$, $\mathbf{1}_{--}$, and $\mathbf{2}$, respectively. The multiplication of the singlets is simply given by

$$\mathbf{1}_{x_1 y_1} \times \mathbf{1}_{x_2 y_2} = \mathbf{1}_{x_3 y_3} \tag{A1}$$

where $x_3 = x_1 x_2$ and $y_3 = y_1 y_2$. While the tensor product for two doublets, $\mathbf{a} = (a_1, a_2)^T$ and $\mathbf{b} = (b_1, b_2)^T$, is

$$\begin{aligned} \mathbf{a} \times \mathbf{b} &= (a_1 b_2 + a_2 b_1)_{\mathbf{1}_{++}} + (a_1 b_2 - a_2 b_1)_{\mathbf{1}_{--}} \\ &\quad + (a_1 b_1 + a_2 b_2)_{\mathbf{1}_{+-}} + (a_1 b_1 - a_2 b_2)_{\mathbf{1}_{-+}}. \end{aligned} \tag{A2}$$

References

1. S.F. King, C. Luhn, Neutrino mass and mixing with discrete symmetry. Rep. Prog. Phys. **76**, 056201 (2013). arXiv:1301.1340 [hep-ph]
2. G. Altarelli, F. Feruglio, Discrete flavor symmetries and models of neutrino mixing. Rev. Mod. Phys. **82**, 2701–2729 (2010). arXiv:1002.0211 [hep-ph]
3. H. Ishimori, T. Kobayashi, H. Ohki, Y. Shimizu, H. Okada, M. Tanimoto, Non-Abelian discrete symmetries in particle physics. Prog. Theor. Phys. Suppl. **183**, 1–163 (2010). arXiv:1003.3552 [hep-th]
4. S.F. King, Models of neutrino mass, mixing and CP violation. J. Phys. G **42**, 123001 (2015). arXiv:1510.02091 [hep-ph]
5. P.H. Frampton, T.W. Kephart, Simple nonAbelian finite flavor groups and fermion masses. Int. J. Mod. Phys. A **10**, 4689–4704 (1995). arXiv:hep-ph/9409330
6. W. Grimus, L. Lavoura, A discrete symmetry group for maximal atmospheric neutrino mixing. Phys. Lett. B **572**, 189–195 (2003). arXiv:hep-ph/0305046
7. W. Grimus, A.S. Joshipura, S. Kaneko, L. Lavoura, M. Tanimoto, Lepton mixing angle $\theta_{13} = 0$ with a horizontal symmetry D_4. JHEP **07**, 078 (2004). arXiv:hep-ph/0407112
8. M. Frigerio, S. Kaneko, E. Ma, M. Tanimoto, Quaternion family symmetry of quarks and leptons. Phys. Rev. D **71**, 011901 (2005). arXiv:hep-ph/0409187
9. A. Blum, C. Hagedorn, M. Lindner, Fermion masses and mixings from dihedral flavor symmetries with preserved subgroups. Phys. Rev. D **77**, 076004 (2008). arXiv:0709.3450 [hep-ph]
10. A. Adulpravitchai, A. Blum, C. Hagedorn, A supersymmetric D4 model for mu-tau symmetry. JHEP **03**, 046 (2009). arXiv:0812.3799 [hep-ph]
11. H. Ishimori, T. Kobayashi, H. Ohki, Y. Omura, R. Takahashi, M. Tanimoto, D(4) flavor symmetry for neutrino masses and mixing. Phys. Lett. B **662**, 178–184 (2008). arXiv:0802.2310 [hep-ph]
12. C. Hagedorn, R. Ziegler, $\mu - \tau$ symmetry and charged lepton mass hierarchy in a supersymmetric D_4 model. Phys. Rev. D **82**, 053011 (2010). arXiv:1007.1888 [hep-ph]
13. D. Meloni, S. Morisi, E. Peinado, Stability of dark matter from the D4xZ2 flavor group. Phys. Lett. B **703**, 281–287 (2011). arXiv:1104.0178 [hep-ph]
14. V.V. Vien, H.N. Long, The D_4 flavor symmery in 3-3-1 model with neutral leptons. Int. J. Mod. Phys. A **28**, 1350159 (2013). arXiv:1312.5034 [hep-ph]
15. V.V. Vien, H.N. Long, Quark masses and mixings in the 3-3-1 model with neutral leptons based on D_4 flavor symmetry. J. Korean Phys. Soc. **66**(12), 1809–1815 (2015). arXiv:1408.4333 [hep-ph]
16. V.V. Vien, Neutrino mass and mixing in the 3-3-1 model with neutral leptons based on D4 flavor symmetry. Mod. Phys. Lett. A **29**, 1450122 (2014)
17. A.E. Cárcamo Hernández, C.O. Dib, U.J. Saldaña Salazar, When $\tan\beta$ meets all the mixing angles. Phys. Lett. B**809**, 135750 (2020). arXiv:2001.07140 [hep-ph]
18. V.V. Vien, Fermion mass and mixing in the $U(1)_{B-L}$ extension of the standard model with D_4 symmetry. J. Phys. G **47**(5), 055007 (2020)
19. V.V. Vien, Fermion mass hierarchies and mixings in a $B-L$ model with $D_4 \times Z_4 \times Z_2$ symmetry. arXiv:2111.14701 [hep-ph]
20. C. Bonilla, L.M.G. de la Vega, R. Ferro-Hernandez, N. Nath, E. Peinado, Neutrino phenomenology in a left-right D_4 symmetric model. Phys. Rev. D **102**(3), 036006 (2020). arXiv:2003.06444 [hep-ph]
21. P. Athron, C. Balázs, D.H.J. Jacob, W. Kotlarski, D. Stöckinger, H. Stöckinger-Kim, New physics explanations of a_μ in light of the FNAL muon g-2 measurement. JHEP **09**, 080 (2021). arXiv:2104.03691 [hep-ph]
22. J.W.F. Valle, M. Singer, Lepton number violation with quasi dirac neutrinos. Phys. Rev. D **28**, 540 (1983)
23. F. Pisano, V. Pleitez, An SU(3) x U(1) model for electroweak interactions. Phys. Rev. D**46**, 410–417 (1992). arXiv:hep-ph/9206242
24. P.H. Frampton, Chiral dilepton model and the flavor question. Phys. Rev. Lett. **69**, 2889–2891 (1992)
25. R. Foot, H.N. Long, T.A. Tran, $SU(3)_L \otimes U(1)_N$ and $SU(4)_L \otimes U(1)_N$ gauge models with right-handed neutrinos. Phys. Rev. D **50**(1), R34–R38 (1994). arXiv:hep-ph/9402243
26. H.N. Long, The 331 model with right handed neutrinos. Phys. Rev. D **53**, 437–445 (1996). arXiv:hep-ph/9504274
27. A.E. Carcamo Hernandez, R. Martinez, F. Ochoa, Z and Z' decays with and without FCNC in 331 models. Phys. Rev. D **73**, 035007 (2006). arXiv:hep-ph/0510421
28. D. Chang, H.N. Long, Interesting radiative patterns of neutrino mass in an SU(3)(C) x SU(3)(L) x U(1)(X) model with right-handed neutrinos. Phys. Rev. D **73**, 053006 (2006). arXiv:hep-ph/0603098
29. A.E. Carcamo Hernandez, R. Martinez, F. Ochoa, Radiative seesaw-type mechanism of quark masses in $SU(3)_C \otimes SU(3)_L \otimes U(1)_X$. Phys. Rev. D **87**(7), 075009 (2013). arXiv:1302.1757 [hep-ph]
30. A.E. Cárcamo Hernández, R. Martinez, F. Ochoa, Fermion masses and mixings in the 3-3-1 model with right-handed neutrinos based on the S_3 flavor symmetry. Eur. Phys. J. C**76**(11), 634 (2016). arXiv:1309.6567 [hep-ph]
31. S.M. Boucenna, S. Morisi, J.W.F. Valle, Radiative neutrino mass in 3-3-1 scheme. Phys. Rev. D **90**(1), 013005 (2014). arXiv:1405.2332 [hep-ph]
32. A.E. Cárcamo Hernández, E. Cataño Mur, R. Martinez, Lepton masses and mixing in $SU(3)_C \otimes SU(3)_L \otimes U(1)_X$ models with a S_3 flavor symmetry. Phys. Rev. D **90**(7), 073001 (2014). arXiv:1407.5217 [hep-ph]
33. A.E. Cárcamo Hernández, R. Martinez, J. Nisperuza, S_3 discrete group as a source of the quark mass and mixing pattern in 331 models. Eur. Phys. J. C **75**(2), 72 (2015). arXiv:1401.0937 [hep-ph]
34. H. Okada, N. Okada, Y. Orikasa, Radiative seesaw mechanism in a minimal 3-3-1 model. Phys. Rev. D **93**(7), 073006 (2016). arXiv:1504.01204 [hep-ph]
35. A.E. Cárcamo Hernández, H.N. Long, V.V. Vien, A 3-3-1 model with right-handed neutrinos based on the $\Delta(27)$ family symmetry. Eur. Phys. J. C **76**(5), 242 (2016). arXiv:1601.05062 [hep-ph]
36. R.M. Fonseca, M. Hirsch, A flipped 331 model. JHEP **08**, 003 (2016). arXiv:1606.01109 [hep-ph]
37. A.E. Cárcamo Hernández, S. Kovalenko, H.N. Long, I. Schmidt, A variant of 3-3-1 model for the generation of the SM fermion

mass and mixing pattern. JHEP**07**, 144 (2018). arXiv:1705.09169 [hep-ph]
38. A.E. Cárcamo Hernández, H.N. Long, V.V. Vien, The first $\Delta(27)$ flavor 3-3-1 model with low scale seesaw mechanism. Eur. Phys. J. C **78**(10), 804 (2018). arXiv:1803.01636 [hep-ph]
39. A.E. Cárcamo Hernández, Y. Hidalgo Velásquez, N.A. Pérez-Julve, A 3-3-1 model with low scale seesaw mechanisms. Eur. Phys. J. C **79**(10), 828 (2019). arXiv:1905.02323 [hep-ph]
40. A.E. Cárcamo Hernández, N.A. Pérez-Julve, Y. Hidalgo Velásquez, Fermion masses and mixings and some phenomenological aspects of a 3-3-1 model with linear seesaw mechanism. Phys. Rev. D **100**(9), 095025 (2019). arXiv:1907.13083 [hep-ph]
41. A.E. Cárcamo Hernández, D.T. Huong, H.N. Long, Minimal model for the fermion flavor structure, mass hierarchy, dark matter, leptogenesis, and the electron and muon anomalous magnetic moments. Phys. Rev. D **102**(5), 055002 (2020). arXiv:1910.12877 [hep-ph]
42. A.E. Cárcamo Hernández, Y. Hidalgo Velásquez, S. Kovalenko, H.N. Long, N.A. Pérez-Julve, V.V. Vien, Fermion spectrum and $g-2$ anomalies in a low scale 3-3-1 model. Eur. Phys. J. C **81**(2), 191 (2021). arXiv:2002.07347 [hep-ph]
43. A.E. Cárcamo Hernández, J.W.F. Valle, C.A. Vaquera-Araujo, Simple theory for scotogenic dark matter with residual matter-parity. Phys. Lett. B **809**, 135757 (2020). arXiv:2006.06009 [hep-ph]
44. Z.-Z. Xing, Flavor structures of charged fermions and massive neutrinos. Phys. Rep. **854**, 1–147 (2020). arXiv:1909.09610 [hep-ph]
45. Particle Data Group Collaboration, P.A. Zyla et al., Review of particle physics. PTEP**2020**(8), 083C01 (2020)
46. I. Esteban, M.C. Gonzalez-Garcia, M. Maltoni, T. Schwetz, A. Zhou, The fate of hints: updated global analysis of three-flavor neutrino oscillations. JHEP **09**, 178 (2020). arXiv:2007.14792 [hep-ph]
47. S. Roy Choudhury, S. Hannestad, Updated results on neutrino mass and mass hierarchy from cosmology with Planck, likelihoods. JCAP **2007**(2020), 037 (2018). arXiv:1907.12598 [astro-ph.CO]
48. M.A. Shifman, A.I. Vainshtein, M.B. Voloshin, V.I. Zakharov, Low-energy theorems for higgs boson couplings to photons. Sov. J. Nucl. Phys. **30**, 711–716 (1979)
49. M.B. Gavela, G. Girardi, C. Malleville, P. Sorba, A nonlinear R(xi) Gauge condition for the electroweak SU(2) X U(1) model. Nucl. Phys. B **193**, 257–268 (1981)
50. P. Kalyniak, R. Bates, J.N. Ng, Two photon decays of scalar and pseudoscalar bosons in supersymmetry. Phys. Rev. D **33**, 755 (1986)
51. M. Spira, QCD effects in Higgs physics. Fortsch. Phys. **46**, 203–284 (1998). arXiv:hep-ph/9705337
52. A. Djouadi, The anatomy of electro-weak symmetry breaking. II. The Higgs bosons in the minimal supersymmetric model. Phys. Rep. **459**, 1–241 (2008). arXiv:hep-ph/0503173
53. W.J. Marciano, C. Zhang, S. Willenbrock, Higgs decay to two photons. Phys. Rev. D **85**, 013002 (2012). arXiv:1109.5304 [hep-ph]
54. L. Wang, X.-F. Han, The recent Higgs boson data and Higgs triplet model with vector-like quark. Phys. Rev. D **86**, 095007 (2012). arXiv:1206.1673 [hep-ph]
55. C.M.S. Collaboration, A.M. Sirunyan et al., Measurements of Higgs boson properties in the diphoton decay channel in proton-proton collisions at $\sqrt{s} = 13$ TeV. JHEP **11**, 185 (2018). arXiv:1804.02716 [hep-ex]
56. ATLAS Collaboration, G. Aad et al., Combined measurements of Higgs boson production and decay using up to 80 fb^{-1} of proton-proton collision data at $\sqrt{s} = 13$ TeV collected with the ATLAS experiment. Phys. Rev. D **101**(1), 012002 (2020). arXiv:1909.02845 [hep-ex]
57. R.A. Diaz, R. Martinez, J.A. Rodriguez, Phenomenology of lepton flavor violation in 2HDM(3) from (g-2)(mu) and leptonic decays. Phys. Rev. D **67**, 075011 (2003). arXiv:hep-ph/0208117
58. F. Jegerlehner, A. Nyffeler, The muon g-2. Phys. Rep. **477**, 1–110 (2009). arXiv:0902.3360 [hep-ph]
59. C. Kelso, H.N. Long, R. Martinez, F.S. Queiroz, Connection of $g-2_\mu$, electroweak, dark matter, and collider constraints on 331 models. Phys. Rev. D **90**(11), 113011 (2014). arXiv:1408.6203 [hep-ph]
60. M. Lindner, M. Platscher, F.S. Queiroz, A call for new physics: the muon anomalous magnetic moment and lepton flavor violation. Phys. Rep. **731**, 1–82 (2018). arXiv:1610.06587 [hep-ph]
61. K. Kowalska, E.M. Sessolo, Expectations for the muon g-2 in simplified models with dark matter. JHEP **09**, 112 (2017). arXiv:1707.00753 [hep-ph]
62. K. Hagiwara, R. Liao, A.D. Martin, D. Nomura, T. Teubner, $(g-2)_\mu$ and $\alpha(M_Z^2)$ re-evaluated using new precise data. J. Phys. **G38**, 085003 (2011). arXiv:1105.3149 [hep-ph]
63. M. Davier, A. Hoecker, B. Malaescu, Z. Zhang, Reevaluation of the hadronic vacuum polarisation contributions to the Standard Model predictions of the muon $g-2$ and $\alpha(m_Z^2)$ using newest hadronic cross-section data. Eur. Phys. J. C **77**(12), 827 (2017). arXiv:1706.09436 [hep-ph]
64. RBC, UKQCD Collaboration, T. Blum, P.A. Boyle, V. Gülpers, T. Izubuchi, L. Jin, C. Jung, A. Jüttner, C. Lehner, A. Portelli, J.T. Tsang, Calculation of the hadronic vacuum polarization contribution to the muon anomalous magnetic moment. Phys. Rev. Lett. **121**(2), 022003 (2018). arXiv:1801.07224 [hep-lat]
65. A. Keshavarzi, D. Nomura, T. Teubner, Muon $g-2$ and $\alpha(M_Z^2)$: a new data-based analysis. Phys. Rev. D **97**(11), 114025 (2018). arXiv:1802.02995 [hep-ph]
66. T. Nomura, H. Okada, One-loop neutrino mass model without any additional symmetries. Phys. Dark Univ. **26**, 100359 (2019). arXiv:1808.05476 [hep-ph]
67. T. Nomura, H. Okada, Zee-Babu type model with $U(1)_{L_\mu-L_\tau}$ gauge symmetry. Phys. Rev. D **97**(9), 095023 (2018). arXiv:1803.04795 [hep-ph]
68. T. Aoyama et al., The anomalous magnetic moment of the muon in the Standard Model. Phys. Rep. **887**, 1–166 (2020). arXiv:2006.04822 [hep-ph]
69. Muon g-2 Collaboration, B. Abi et al., Measurement of the positive muon anomalous magnetic moment to 0.46 ppm. Phys. Rev. Lett. **126**(14), 141801 (2021). arXiv:2104.03281 [hep-ex]
70. F.S. Queiroz, C. Siqueira, J.W.F. Valle, Constraining flavor changing interactions from LHC run-2 dilepton bounds with vector mediators. Phys. Lett. B **763**, 269–274 (2016). arXiv:1608.07295 [hep-ph]
71. A. Dedes, A. Pilaftsis, Resummed effective Lagrangian for Higgs mediated FCNC interactions in the CP violating MSSM. Phys. Rev. D **67**, 015012 (2003). arXiv:hep-ph/0209306
72. A. Aranda, C. Bonilla, J.L. Diaz-Cruz, Three generations of Higgses and the cyclic groups. Phys. Lett. B **717**, 248–251 (2012). arXiv:1204.5558 [hep-ph]
73. S. Khalil, S. Salem, Enhancement of $H \to \gamma\gamma$ in $SU(5)$ model with 45_{H^1} plet. Nucl. Phys. B **876**, 473–492 (2013). arXiv:1304.3689 [hep-ph]
74. A.J. Buras, F. De Fazio, 331 models facing the tensions in $\Delta F = 2$ processes with the impact on ε'/ε, $B_s \to \mu^+\mu^-$ and $B \to K^*\mu^+\mu^-$. JHEP **08**, 115 (2016). arXiv:1604.02344 [hep-ph]
75. P.M. Ferreira, I.P. Ivanov, E. Jiménez, R. Pasechnik, H. Serôdio, CP4 miracle: shaping Yukawa sector with CP symmetry of order four. JHEP **01**, 065 (2018). arXiv:1711.02042 [hep-ph]
76. N.T. Duy, T. Inami, D.T. Huong, Physical constraints derived from FCNC in the 3-3-1-1 model. Eur. Phys. J. C **81**, 813 (2021). arXiv:2009.09698 [hep-ph]